

Adaptive Internal Model of Intrinsic Kinematics  
Involved in Learning an Aiming Task

Hiroshi Imamizu,  
Yoji Uno,  
and  
Mitsuo Kawato

ATR Human Information Processing  
Research Laboratories

Address correspondence to:

Hiroshi Imamizu  
Kawato Dynamic Brain Project  
Japan Science and Technology Corporation  
2-2, Hikaridai, Seika-cho, Soraku-gun, Kyoto 619-02, Japan  
Telephone: +81-774-95-1220  
Facsimile: +81-774-95-3001  
E-mail: [imamizu@erato.atr.co.jp](mailto:imamizu@erato.atr.co.jp)

Running head: Adaptive Internal Model of Intrinsic Kinematics

### Abstract

We multiplied the elbow joint angle and the shoulder joint angle of participants aiming at targets in an experiment using a position recording system and a CRT screen. The linear transformation in joint angles (intrinsic coordinates) involved in the experiment corresponded to a nonlinear transformation between the hand coordinates and the screen coordinates (extrinsic coordinates). The present study examined whether the participants could learn this transformation in the intrinsic coordinates or in the extrinsic coordinates, by investigating intermanual (between-hands) transfer under an intrinsically-consistent condition and under an extrinsically-consistent condition. The participants learned to adjust for the transformation in the first stage for both conditions. In the second stage under the intrinsically-consistent condition, the participants learned to adjust for the same transformation in the intrinsic coordinates as that in the first stage. Likewise, in the second stage under the extrinsically-consistent condition, they learned to adjust for the same transformation in the extrinsic coordinates as that in the first stage. Positive intermanual transfer was observed under the intrinsically-consistent condition but not under the extrinsically-consistent condition. Results suggest that participants can learn the linear transformation in joint angles in the intrinsic coordinates and that the central nervous system adaptively represents the intrinsic kinematics.

## Introduction

In everyday life, people interact continuously with objects in extra-personal space. Reaching movements— e.g., bringing a hand to the location of an object—are fundamental behaviors by means of which we interact with the external world. Because of this, the study of reaching movements has received a great deal of interest. Recent advances in computational models of the complex mechanisms underlying reaching movements have provided a comprehensive account of how a purposeful act may be planned and executed from sensory input to motor output in the central nervous system (CNS). Some computational studies have suggested that the motor system contains an internal representation of the geometry of the limbs, such as muscle lengths or joint angles, to control movement. Whether the geometric aspects of motion (kinematics) are adaptively represented in the CNS in intrinsic space is examined in the present study, by an investigation of intermanual transfer in the learning of an aiming task under different conditions.

### A Hierarchical and a Non-Hierarchical Model of Visually-Guided Movements

Many computational models have been proposed for visually-guided reaching movements. These models can be divided into two classes depending on their approach. One approach is to divide the problem of "control of visually-guided movements" into several sub-processes and solve each of the sub-processes in a hierarchical manner analogous to that used in the control of robot arms (Hollerbach, 1982; Saltzman, 1979; Saltzman & Kelso, 1987). The other approach is based on a non-hierarchical method that translates a sensory stimulus directly into time-varying patterns of muscular activation (Massone & Bizzi, 1989).

To provide a comprehensive example of the hierarchical model, the upper row in Figure 1 schematically illustrates a computational model based on the former approach, and the lower rows in the figure show hierarchical levels of coordinate reference frames used in the control of a robot arm. During reaching tasks, the target position is usually identified visually, resulting in a representation in the CNS in terms of visual space (extrinsic space). In the present study, Cartesian coordinates were assumed, in which the origin is at the center of the shoulder, consistent with assumptions of previous computational studies (Atkeson, 1989; Hollerbach, 1990). The position information represented in such a space, however, is not directly linked to parameters of the motor apparatus (i.e., joint angle and torque) and must be translated into these coordinates (intrinsic space).

The first problem is translation from extrinsic space to intrinsic space, and is referred to as a coordinate transformation. In the model illustrated in Figure 1, the target location is translated into joint angle space. The second problem is determination of a trajectory from the current position to the target and is termed trajectory planning. The last problem is computation of the joint torque necessary to obtain the planned trajectory, that is, geometric properties of motion (kinematics). The planned trajectory must be translated into dynamic properties of the motor apparatus related to the force required to complete the motion (dynamics). This is called the control problem.

-----  
 Insert Figure 1 about here  
 -----

Although the reference frames of motion mentioned above (i.e., Cartesian space, joint angle space, and joint torque space) are often used in the control of a robot arm, it is unlikely that these frames are used in the CNS. Nevertheless, there are parameters that are known to be perceived in the CNS that are functionally equivalent to these artificial

frames. For example, the parameters of joint angle and torque are closely related to muscle length and tension, respectively.

A non-hierarchical approach to modeling visually-guided reaching movements was proposed by Massone and Bizzi (1989). They proposed a neural network model of a sensory-motor transformation that translates a sensory stimulus directly into time-varying patterns of muscular activation. Figure 2 shows a schematic diagram of their model and a simplified architecture of the proposed network. The input for the network is sensory stimulation representing the target location in extrinsic space and the output is a time-varying trajectory in muscle space (i.e., motor commands in intrinsic space). This model does not require intermediate representations (i.e., the target location in intrinsic space or the trajectory in intrinsic space), which are required in the hierarchical model.

-----  
 Insert Figure 2 about here  
 -----

The classes of models underscore the current controversy in neuroscience regarding how movement is controlled in the CNS—whether in a hierarchical or non-hierarchical manner. Although a hierarchical approach provides an exact and comprehensive account of actual problems associated with motor control, several neurophysiologists (e.g., Alexander, DeLong, & Crutcher, 1992; Kalaska & Crammond, 1992) have pointed out that such sequential and analytic approaches give implausible accounts of how movement is controlled in the CNS.

Three problems—coordinate transformation, trajectory planning, and control—must be solved to bring the hand from the starting position to the target for the following reasons. First, the coordinate system used in the visual system is different from that used in the motor system. Thus, a coordinate transformation is necessary to link sensory input to motor output. Second, it is well-known that the hand's trajectory between any two

points has some invariant properties—the hand’s path is roughly straight and the hand’s speed-profiles are bell-shaped (Abend, Bizzi, & Morasso, 1982; Morasso, 1981). These invariant properties suggest that the trajectories are planned in the CNS according to some optimization principles (Flash & Hogan, 1985; Uno, Kawato, & Suzuki, 1989). Third, the fact that the hand rapidly and smoothly moves to the target suggests that the arm is successfully controlled taking its dynamic properties into account. It is not clear, however, whether these problems are sequentially — hierarchically — solved using several modules or simultaneously — non-hierarchically — solved using one module.

#### Internal Representation of Intrinsic Kinematics

The goal of the present study is to investigate whether a representation of intrinsic kinematics is used during the control of visually-guided movements in the CNS and whether this representation changes during the learning of an aiming task in which the visual feedback has been altered with a transform function. The hierarchical model of visually-guided movements predicts that an intermediate representation of intrinsic kinematics is formed between the computational modules (Figure 1), whereas the non-hierarchical model does not require such a representation (Figure 2). Thus, the presence of a representation of intrinsic kinematics in the CNS would support the hierarchical model rather than the non-hierarchical model of visually-guided reaching movements.

It is worth noting that the presence of such representation does not reject the network model proposed by Massone and Bizzi (1989) because there is a possibility that some neurons (computational elements) in the model might come to represent the intrinsic kinematics by chance after the training of the network. However, the presence of such neurons would indicate that the coordinates transformation is solved before these neurons are activated and that the control problem is solved afterwards. This suggests that the

model is hierarchical. In other words, the representation of the intrinsic kinematics makes the model hierarchical.

Some sources of evidence supporting the idea that the CNS contains representations of intrinsic kinematics have emerged through recent neurophysiological studies on multi-joint behavioral tasks. Kalaska and his co-workers showed that the activity of the proximal-arm-related neurons in the superior parietal lobule (Brodmann area 5) of monkeys continuously changes depending on the direction of arm movements (Kalaska, Caminiti, & Georgopoulos, 1983), and this activity was not affected by an external load on the arm in various directions (Kalaska, Cohen, Prud'homme, & Hyde, 1990). The authors concluded that area 5 neurons encode movement kinematics, not movement dynamics. Lacquaniti, Guigon, Bianchi, Ferraina, and Caminiti (in press) reported that an intrinsic coordinate system centered at the shoulder and defined by the elevation and azimuth angles of the proximal arm (i.e., shoulder-joint configuration) and by the angle of extension at the elbow, provides a better account of neural modulation in area 5 than an extrinsic coordinate system does (Cartesian coordinate system parallel to the laboratory frame). These data suggest that proximal-arm-related neurons encode the intrinsic kinematics of arm movements and that area 5 is involved in the integration of this sensory and motor information.

In this research we investigated whether a representation of intrinsic kinematics is used in the control of reaching movements using a behavioral paradigm in which visual feedback of the hand position of participants was altered with a transform function based on multiplication of the shoulder-joint and elbow-joint angles by constant values during an aiming task. If a representation of intrinsic kinematics in the CNS is used in the control of arm movements, then an adjustment to this transform would be learned in terms of the intrinsic space. However, if a representation of intrinsic kinematics is not used, then the adjustment would not be learned or would be learned using another mechanism, perhaps in

terms of extrinsic space. As mentioned above, it is unlikely that joint angles are represented in the CNS. However, parameters that are functionally equivalent to joint angles might be represented using information from sensory receptors within the muscles, tendons, joints, and skin (i.e., proprioception; Rosenbaum, 1991).

### Visual-Motor Learning Under Transformed Visual Feedback

Many investigators have studied the learning of motor tasks (e.g., reaching, aiming, and drawing) under transformed visual feedback to investigate how the relation between visual information and motor commands is learned. In some studies, the visual feedback was transformed using an optical device such as a prism or a mirror. Experimental paradigms using such devices are called prism adaptation (Held & Gottlieb, 1958) or mirror drawing (Cook, 1933). Other studies have used a position recording system, such as a digitizing tablet and CRT screen controlled by a computer (Fig. 3), to process the recorded position through a transform function before display (Cunningham, 1989; Imamizu & Shimojo, 1995).

-----  
 Insert Figure 3 about here  
 -----

The majority of these studies have reported that participants who were initially exposed to transformed visual feedback made large errors in the motor task and that the errors decreased as the number of trials increased. Some of the studies revealed important facts concerning the nature of the adaptation to (or the adjustment to) the transformed visual feedback: 1) adaptation to the transformed visual feedback causes subsequent errors under normal visual feedback. This phenomenon, called an aftereffect, can be observed even when participants are informed of the return to normal visual feedback, suggesting that the adaptation is not entirely under conscious control (Welch, 1978). 2)

Milner, Corkin, and Teuber (1968) reported that a patient who had a deficit in verbal and cognitive memory because of brain damage could learn a mirror drawing task, and that the learning was stable for a long period. 3) Held and Hein (1958) compared two conditions of prism adaptation: with active or passive arm movement. The participants either swung the arm back and forth in the frontal plane (active movement) or had it transported in the same manner by means of a moving "cradle" to which it was strapped (passive movement). They found that the active movement produced adaptation, whereas the passive movement did not.

These features of visual-motor learning under transformed visual feedback (i.e., some degree of independence from conscious control and cognitive memory and the requirement of active movements during the training period) suggest that it is like other kinds of motor learning, such as skill acquisition in the playing of sports or musical instruments. The advantage of experimental paradigms using transformed visual feedback is that the learning process can be investigated using reaching or aiming tasks that have a clear objective (i.e., to bring the hand to the exact location of an object) and is well-suited for studying the translation of sensory input to motor output in the CNS.

Although a similar experimental paradigm of visual-motor learning under transformed visual feedback was used in the present study, there is a critical difference between previous research and the present study. In previous research, the positions of the participant's hand and objects in the visual field were altered by a transform function expressed simply in the task-oriented extrinsic coordinates (denoted by  $f$  in Fig. 4). For example, in prism adaptation, the hand and object positions were "translated" and in mirror drawing, the positions were "reflected." In the present study, however, a transform function that can be expressed simply in intrinsic coordinates was used (denoted by  $g$  in Fig. 4); a "magnification" of the joint angles.

---

Insert Figure 4 about here

-----

A transform function represented in extrinsic coordinates can be translated into one that is represented in intrinsic coordinates, or vice versa; however, a transform function that is simple (e.g., translation or reflection) in extrinsic coordinates becomes complicated in intrinsic coordinates, and vice versa. This is because the relationship between extrinsic and intrinsic coordinates is complex and nonlinear. This relation is discussed in detail at the end of the next section.

### Linear Transformation of Joint Angles

The kinematics of a two-link arm moving in a horizontal plane, as illustrated in Figure 3, is usually expressed as follows:

$$\begin{aligned} p &= l_1 \cos \theta_1 + l_2 \cos(\theta_1 + \theta_2) \\ q &= l_1 \sin \theta_1 + l_2 \sin(\theta_1 + \theta_2), \end{aligned} \quad (1)$$

where  $(p, q)$  represents the hand position in the horizontal plane (i.e., the surface of a board above which the hand moves) and  $\theta_1$  and  $\theta_2$  denote the shoulder-joint angle and elbow-joint angle (Fig. 3) respectively.  $l_1$  and  $l_2$  are the upper arm and forearm length respectively.

Figure 5 illustrates the linear transformation of joint angles used in the present study.  $P(p, q)$  represents the hand position in the horizontal plane (i.e., surface of the board above which the hand moves), while  $X(x, y)$  represents the cursor position on the CRT screen. The cursor position was determined so that a mapping in joint angles is represented as

$$\begin{aligned} \theta_1^* &= 1.25(\theta_1 - h_1) + h_1 \\ \theta_2^* &= 0.5(\theta_2 - h_2) + h_2, \end{aligned} \quad (2)$$

where  $(h_1, h_2)$  is a fixed point for this mapping.  $\theta_1^*$  and  $\theta_2^*$  denote the shoulder-joint angle and elbow-joint angles of a transformed arm configuration (not visible in the display shown to participants) shown in the top portion of Figure 5; that is,

$$\begin{aligned} x &= l_1 \cos \theta_1^* + l_2 \cos(\theta_1^* + \theta_2^*) \\ y &= l_1 \sin \theta_1^* + l_2 \sin(\theta_1^* + \theta_2^*). \end{aligned} \quad (3)$$

Thus, Equation 3 represents the magnification of the shoulder-joint angle and minimization of the elbow-joint angle.

-----  
 Insert Figure 5 about here  
 -----

It should be noted that this linear transform of intrinsic coordinates corresponds to a nonlinear transform function of extrinsic coordinates. The relation between the hand position  $P(p, q)$  and the cursor position  $X(x, y)$  on the CRT screen was obtained by rearranging Equations (1), (2), and (3) so as to eliminate the intrinsic parameters (i.e.,  $\theta_1$ ,  $\theta_2$ ,  $\theta_1^*$  and  $\theta_2^*$ ), that is,

$$X = (P). \quad (4)$$

The introduced transform function is nonlinear and highly complex. Figure 6A illustrates the effect of the transform on hand position  $P(p, q)$  in the map of the screen coordinates  $X(x, y)$ . As a participant moves a hand along the straight grid lines (the bottom of Fig. 6A), the cursor trajectories on the CRT screen become curved (the top of Fig. 6A).

-----  
 Insert Figure 6 about here  
 -----

-----

### Testing Whether Participants Learn to Adjust for the Transform in terms of the Intrinsic Space

Because the purpose of the present study was to determine whether a model corresponding to the artificial transformation of joint angles is represented in the CNS in terms of the internal kinematics, it was critical that participants learn to adjust for the transformation either in terms of joint angles (i.e., intrinsic coordinates) or in terms of hand and screen coordinates (i.e., extrinsic coordinates). If there is a representation of the intrinsic kinematics in the CNS and this representation is adaptive, then the participants should learn to adjust for the transformation in terms of the intrinsic coordinates.

Alternatively, if there is no internal representation of the intrinsic kinematics or if the representation is not plastic, the participants should learn the nonlinear and complicated mapping of using the hand  $p - q$  coordinates and the screen  $x - y$  coordinates.

We examined whether participants learned to adjust for a transformation of joint angles in intrinsic coordinates or in extrinsic coordinates using two experimental conditions, i.e., an extrinsically-consistent condition and an intrinsically-consistent condition. Each of the conditions consisted of two successive stages of learning. The participants executed an aiming task using different arms in the two stages. The joint angles were transformed by Equation 2 in the first stage for both conditions.

Under the extrinsically-consistent condition (Figures 6A and 6B) in the second stage, the participants executed the aiming task under the same mapping between the screen coordinates and the hand coordinates as that in the first stage using their other arm (compare the top of Figure 6A to that of Figure 6B). Although the mapping in the second stage was the same in the extrinsic coordinates as that in the first stage, it was quite different in the intrinsic coordinates (in terms of joint angles) because the arm used by the participants in the first stage was different from the arm used in the second stage.

The bottom of Figure 6B illustrates the meaning of the transformation used in the second stage under the extrinsically-consistent condition in the intrinsic coordinates. When the hand and the elbow are located in the horizontal plane at the level of the shoulder, the other geometrically possible arm configuration appears, whose forearm length, upper arm length and positions of the shoulder and hand are the same as those of the original configuration, as indicated by the broken lines in the figure; in general, however, it is biologically impossible because of the limitations of the joint angles. The transformation in the second stage corresponded to that of the joint angles ( $\theta_1$  and  $\theta_2$  in the figure) of the biologically impossible arm configuration instead of the actual arm configuration.

Under the intrinsically-consistent condition, the participants executed the aiming task under a different mapping between the screen and the hand coordinates in the second stage from that in the first stage. The mapping in the second stage was symmetric to that in the first stage with respect to the y-axis (compare the top of Figure 6A to that of Figure 6C). However, the two mappings corresponded to the same transformation of joint angles in the intrinsic coordinates, because the arm used by the participants in the first stage was different from the arm used in the second stage (compare the bottom of Figure 6A to that of Figure 6C).

Therefore, we can predict the two simplest results depending on whether the participants learn to adjust for the transformation of the joint angles in extrinsic coordinates, i.e., the nonlinear mapping between the hand coordinates and the screen coordinates, or in intrinsic coordinates in the first stage. On the one hand, if the participants learn to adjust for the transformation in extrinsic coordinates in the first stage, then a larger positive intermanual transfer of the learning effect would be observed under the extrinsically-consistent condition than under the intrinsically-consistent condition, because the participants would learn the same mapping under the extrinsically-consistent

condition while they would learn mappings that differed under the intrinsically-consistent condition (Fig. 7A). On the other hand, if the participants learn to adjust for the transformation in intrinsic coordinates in the first stages, then a larger positive intermanual transfer would be observed under the intrinsically-consistent condition than under the extrinsically-consistent condition, because they would learn the same intrinsic transformation under the intrinsically-consistent condition while they would learn transformations that differed under the extrinsically-consistent condition (Fig. 7B).

The relation between the transformation in the first stage and that in the second stage under the extrinsically-consistent condition is clear in terms of the intrinsic kinematics when they are represented as transformations of joint angles. The transformation in the first stage is represented as Equation 2 while that in the second stage is represented as

$$\begin{aligned} \theta_1^* &= 1.25 \theta_1 + (1 - 1.25) \theta_1 - h_1 + 2 \cdot 1.25 \arctan \frac{l_2 \sin \theta_2}{l_1 + l_2 \cos \theta_2} \\ &\quad - 2 \arctan \frac{l_2 \sin(0.5 \theta_2 + h_2)}{l_1 + l_2 \cos(0.5 \theta_2 + h_2)} \\ \theta_2^* &= 0.5 \theta_2 + h_2 \end{aligned} \quad (5)$$

using the joint angles of the real arm configuration ( $\theta_1, \theta_2$ ) instead of  $\theta_1$  and  $\theta_2$  (for the full account of the difference in the intrinsic coordinates, see Appendix A).

-----  
 Insert Figure 7 about here  
 -----

## Methods

### Participants

Eight undergraduate students (six women and two men, ranging in age from 17 to 23 years) volunteered to participate. All participants were naive as to the purpose of this experiment and self-reported to be right-handed. They were paid for their participation and were treated in accordance with the "Ethical Principles of Psychologists and Code of Conduct" (American Psychological Association, 1992).

### Apparatus

The participants were seated in a dentist's chair (Nagashima SN-OP) facing a 33-inch CRT screen controlled by a computer (TOSHIBA J3100ZX with a 33 MHz main processor; Fig. 3). The distance between the participants' forehead and the screen was approximately 1.0 m. The participants wore a custom molded cast that immobilized the wrist and a shoulder harness attached to the chair so that the shoulder position was fixed. They moved the arm above a large board (1 m long, 2 m wide, 2 cm thickness) placed horizontally in front of them. The height of the chair was adjusted so that the participants' shoulders were approximately at the level of the board. The participants gripped a vertical rod (10 cm long, 2 cm in diameter) in their palm. One end of the rod was firmly attached to the center of a small light-weight board (10 cm long and wide, 0.5 cm thickness) so that it always stood vertically on the large horizontal board. The participants were instructed to move the rod so that the underside of the small board attached to the rod slid over the top surface of the large board. The large board was covered with a sheet of Teflon to reduce friction. A marker (an infrared light emitting diode) of the position recording system (Northern Digital OPTOTRAK) was attached to the top of the hand-held rod. Its position was sampled at 100 Hz and stored in the computer. The position of the marker was displayed as a movable cursor, i.e., a filled circle 0.9 mm in diameter. The ratio of the marker movement on the board to the cursor movement was approximately 1:1 in all directions when the visual feedback was not altered.<sup>1</sup> A shield was placed above the

board and the participants' hand to eliminate direct vision of the hand and arm. The room was almost completely dark.

### Tasks

Each trial followed a 4-s preparatory phase: a target (a filled circle 5 mm in diameter) and a starting zone (an open circle 5 mm in diameter) appeared on the screen, and the participant moved the cursor into the starting zone. All participants could obtain the target easily within the 4-s interval even under transformed visual feedback. After the end of the preparatory phase, two successive auditory cues (i.e., clicks) were generated by the computer to signal the beginning and the end of each trial. The time interval between the first cue and the second cue was 900 ms. The participants were required to move the cursor as close to the target as possible within this time limit. They were instructed to freeze the movement for a moment after the second cue, and then to move the cursor to the target at any speed. The hand trajectory was analyzed after the onset of the first auditory cue and before the participants momentarily froze the movement.

The test area was determined for each participant considering the physical constraints of the arm configurations as follows: the far border of the test area was a semi-circle centered at the shoulder and with a diameter equal to 85% of each participant's arm length to ensure comfortable and stable arm movements (Fig. 8A). The near border was a straight line 30% of the arm length in front of the shoulder so that the body trunk would not be an obstacle to hand and arm movements. The targets and starting zones were pseudo-randomly located in the test area under the following constraints: 1) the distance between the center of the target and that of the starting zone was less than 65% and more than 32% of each participant's arm length and 2) those positions resulting in cursor positions outside the border of the CRT screen after the transform were excluded. Most locations in the right and the left corners of the test area were excluded for this reason.

Figures 8B and C show the pairs of targets and starting positions in one of the trial blocks in the screen coordinates and in the hand coordinates, respectively.

-----  
 Insert Figure 8 about here  
 -----

While the participant was executing the aiming task, the visual feedback (the cursor position) was altered by a real-time transform function using a microcomputer operation as follows. First, the joint angles ( $\theta_1, \theta_2$ ) were calculated from the position of the marker (p, q) attached to the participant's hand according to the inverse kinematics:

$$\theta_2 = \arccos \frac{p^2 + q^2 - l_1^2 - l_2^2}{2l_1l_2}$$

$$\theta_1 = \arctan \frac{q}{p} - \arctan \frac{l_1 \sin \theta_2}{l_1 + l_2 \cos \theta_2} \quad (6)$$

Thus, the joint angles were not directly measured, but estimated from the marker position (p, q) and the length of each participant's upper arm ( $l_1$ ) and forearm ( $l_2$ ). Second, the joint angles were transformed according to Equation 2. Third, the cursor position (x, y) corresponding to the transformed joint angles ( $\theta_1^*, \theta_2^*$ ) was calculated according to Equation 3. It is difficult to measure the precise length of time required for the computer to complete this operation, but it is estimated to be less than 10 ms, and the participants did not detect a substantial time difference between their hand movement and the cursor movement.

As indicated by Equation 2, deviations of joint angles from constant values ( $h_1, h_2$ ) were multiplied by 1.25 or 0.5. These constant values were determined for each participant so that the hand position (p, q) corresponding to the constant joint angles ( $h_1, h_2$ ) was at approximately the center of the test area, that is, p was 0.0 (straight ahead of the shoulder position), and q was 64% of the arm length. The average of  $h_1$  was

37.69°, ranging from 36.72° to 40.54°, that of  $h_2$  was 100.08°, ranging from 100.00° to 100.15°, and that of  $q$  was 40.74 cm, ranging from 38.57 cm to 43.07 cm.

The above procedure for the cursor alteration is for the transformation of the joint angles in the first stage when the participants used one arm, and it generates the mapping between the hand and the screen coordinates shown in Figure 6A. The transformation in the second stage under the extrinsically-consistent condition when the participants used their other arm is generated by a similar procedure but we use  $\alpha_1$  and  $\alpha_2$  (the shoulder-joint angle and the elbow-joint angle of the other arm configuration whose forearm length, upper arm length and positions of the shoulder and hand are the same as those of the actual configuration: Fig. 6B) instead of  $\alpha_1$  and  $\alpha_2$ , respectively, after calculation of joint angles from the position of the marker. We calculate  $\alpha_1$  and  $\alpha_2$  using the relations:

$$\begin{aligned} \alpha_1 &= \alpha_1 - 2\arctan \frac{l_2 \sin \alpha_2}{l_1 + l_2 \cos \alpha_2} \\ \alpha_2 &= \alpha_2 \end{aligned} \quad (7)$$

(for a full account of these relations, see Appendix A).

### Procedure and Experimental Design

At the beginning of the experiment, the length of the upper arm ( $l_1$ ) and forearm ( $l_2$ ) of each participant were measured. The upper arm length was measured from the shoulder (the tip of the acromial process) to the elbow (the lateral condyle of the humerus), and the forearm length was measured from the elbow to the center of the marker attached to the top end of the rod held in the participant's hand. The average of  $l_1$  was 30.6 cm, ranging from 29.4 cm to 32.3 cm, while that of  $l_2$  was 32.8 cm, ranging from 31.2 cm to 35.5 cm. The transformation of the visual feedback and determination of the positions of

the targets and starting zones were modified according to the arm length of each participant.

After measurement of the arm length, the participants were instructed about the procedure of the task as follows (scripts have been translated to English from Japanese for this report):

A movable cursor represented by a small filled circle, a target represented by a filled circle, and a starting zone represented by an open circle will appear on the screen. Move the cursor into the starting zone, and wait until the computer generates the first auditory cue. After hearing the first cue, please move the cursor as close to the target as possible. Your time limit is 900 ms. At the end of this limit, the computer will generate the second cue. You must immediately freeze your movement for a moment. Then, you can move the cursor to the target at any speed you like.

The participants performed sixteen practice trials under normal conditions (i.e., the mapping between the hand coordinates and the screen coordinates was the identity map):

$$x = p, \quad y = q. \quad (8)$$

The experimenter instructed them to remember the time interval of 900 ms during this practice period.

Following the practice trials, the transformation was described to the participants as follows:

The cursor position on the screen will be transformed as if your shoulder-joint angle is multiplied by 1.25 and your elbow-joint angle is multiplied by 0.5 after the beginning of the next trial. It may be difficult to move the cursor to the target, but you will find that the task will become easier with practice.

The participants were not allowed to experience any trials under transformed visual feedback for practice.

Then, each participant began to learn the aiming task under transformed visual feedback according to the learning schedules shown in Table I. As described earlier, the participants were randomly divided into extrinsically-consistent and intrinsically-consistent groups. All of the participants learned the aiming task using one arm in the first stage while the cursor position was altered according to Equation 2 (Fig. 6A). The participants changed the performing arm in the second stage. The rules on how to alter the cursor position in the second stage was different between the two groups. The cursor position on the screen was altered so that the mapping between the screen coordinates and the hand coordinates would be identical to that in the first stage in the extrinsically-consistent group (Fig. 6B), whereas it was altered so that the transformation of joint angles would be identical to that in the first stage in the intrinsically-consistent group (Fig. 6C). Furthermore, the participants of each group were divided into subgroups: the participants of one subgroup used the right (i.e., preferred) arm in the first stage and the left (i.e., non-preferred) arm in the second stage, while those of the other subgroup used the left arm in the first stage and the right arm in the second stage.

-----  
 Insert Table I about here  
 -----

The test area in the second stage was shifted to the left or right direction so that the center of the test area was directly in front of the shoulder point under both conditions. The shift in the position of the test area may have had some effect on the initial performance of the participants in the second stage, and may have impeded the generalization of the learning effect to the performance in the second stage. The effect was assumed to be minimal because Bedford (1989) reported that respondents wearing

prism spectacles can easily generalize the effect of learning when aiming targets are shifted in the left or right direction.

Each of the stages consisted of 12 trial blocks and lasted about 3 h. Each trial block consisted of 50 trials of the aiming task and lasted about 12 min. A 3 min rest period was allowed between blocks, and a 30 min rest period was allowed between the stages.

The experiment described above takes from seven to eight hours including the measurement of arm lengths and rest time, and was conducted within a single day for each participant. The participant was required to return on an additional day within one week after the experiment to execute 14 trial blocks of the aiming task under normal conditions. They used the right arm in seven trial blocks and the left arm in the remaining seven trial blocks, successively. The data obtained on the second day was used in a linear regression analysis of the aiming error.

### Data analysis

The position of the marker attached to the hand-held rod was sampled at 100 Hz and stored in the computer. Although the position recording system was carefully adjusted before the experiment, it did not detect the position of the marker in some trials. Such trials were called missing trials, and were not included in the analysis described below. The maximum number of missing trials for each stage (600 trials) was eight for any participant.

Aiming error. After the end of the experiment, the end point of the first ballistic movement<sup>2</sup> in each trial of the aiming task was determined using the curvature methods developed by Pollick and Ishimura (1996). Figure 9 illustrates how the end point of the first ballistic movement was detected. The end point of the ballistic movement was

defined as the point where the movement was corrected for the first time. At that point, the tangential velocity is close to zero and the curvature increases markedly. The tangential velocity is defined as  $\sqrt{\dot{p}^2 + \dot{q}^2}$ , where  $\dot{p}$  and  $\dot{q}$  are the instantaneous velocities in the p- and q-coordinates. Figures 9A and B show a typical trajectory in one trial. The curvature (C) at each point in the trajectory was calculated using the equation

$$C = \frac{\dot{p}\ddot{q} + \ddot{p}\dot{q}}{(\dot{p}^2 + \dot{q}^2)^{3/2}}, \quad (9)$$

where  $\ddot{p}$  and  $\ddot{q}$  are the accelerations at that point. The velocity was computed by a fifth-order central difference based on the interpolation polynomial and is defined as

$$\dot{p}_i = \frac{p_{i-2} - 8p_{i-1} + 8p_{i+1} - p_{i+2}}{12 t}, \quad (10)$$

where  $p_i$  is the i-th data value (position of the p-coordinate of the marker), and  $t$  is the time interval between data values.  $t$  was 10 ms because the position was sampled at 100 Hz in this experiment. The acceleration was computed using a similar method and is defined as

$$\ddot{p}_i = \frac{2\dot{p}_{i-2} - \dot{p}_{i-1} - 2\dot{p}_{i+1} + \dot{p}_{i+2}}{7(t)^2}. \quad (11)$$

The velocity and acceleration of the q coordinates were computed in the same manner as those of the p coordinates. In Figure 9C, the velocity and the curvature are plotted as functions of time from the onset of the first auditory cue signalling the beginning of the trial. The end point of the first ballistic movement was defined as the point at which the curvature exceeded  $0.1 \text{ mm}^{-1}$  for the first time after the velocity was maximum. The distance between the center of the target and the end point of the first ballistic movement

was called the aiming error and used as an indicator of learning and the difficulty of the aiming task. The aiming error is expected to decrease with learning and increase with task difficulty.

-----  
 Insert Figure 9 about here  
 -----

The effect of distortion caused by the transformation on the aiming error. The aiming error may be affected by factors other than learning and the difficulty of the task. For example, the aiming error increases as the average velocity of the movement increases, according to Schmidt's law (Schmidt, Zelaznik, Hawkins, Frank, & Quinn, 1979). In the current experiment, the distance between the target and the starting zone was randomly determined for each trial, whereas the movement time was relatively constant, because the participants were required to move the cursor to the target within 900 ms. Thus, the average velocity of the ballistic movement was markedly different from trial to trial.

To exclude the effect of velocity, a linear model of the aiming error was assumed (E):

$$E = aV + b\frac{L}{T} + K \quad (12)$$

and the values of  $a$ ,  $b$ , and  $K$  were estimated using linear regression analysis. Here,  $L$  is the distance between the center of the starting zone and that of the target, and  $T$  is the movement time (i.e., from the onset of the movement to the time when the first ballistic movement terminates) in each trial. The onset of the movement was detected using a method similar to that used for detecting the end point of the first ballistic movement. This was defined as the point where the curvature last dropped below  $0.1 \text{ mm}^{-1}$  before the

velocity reached maximum (Fig. 9C). Note that  $L/T$  equals the average velocity, and the second and third terms on the right side of the equation correspond to Schmidt's law ( $K$  is the constant error). The first term on the right side is specific to this experiment.  $V$  represents the magnitude of distortion caused by the transform (Fig. 10), and is defined as the subtraction of one vector,  $\vec{S}$ , from the other vector,  $\vec{G}$ .  $\vec{G}$  represents the displacement from the target on the hand plane to that on the screen, while  $\vec{S}$  represents the displacement from the starting zone on the hand plane to that on the screen. It is assumed that distortion affects the aiming error (i.e., the error becomes larger as the degree of distortion ( $V$ ) becomes larger) before learning of the aiming task. After learning, however, the error is small, and may become somewhat independent of the degree of distortion. Thus, the value of  $a$  reflects learning and the difficulty of the aiming task independent of the average velocity. The values of  $b$  and  $K$  were estimated using linear regression analysis of the aiming error when the participants aimed at the targets under normal conditions (data obtained on the second day).

-----  
 Insert Figure 10 about here  
 -----

A simple method to investigate the effect of intermanual transfer of learning is to investigate the significant difference between the aiming error in the last block of the first stage and that in the first block of the last stage. However, we compared the values of  $a$  estimated for each of these blocks because the aiming error was possibly affected by the factors described above.

## Results

### Trajectories and Velocity Profiles

Figures 11A and D show the trajectories of the hand coordinates of one participant (K.S.) in the first and the last blocks, respectively, of the first stage under the extrinsically-consistent condition. Figure 11G shows the trajectories in the first block of the second-stage under the extrinsically-consistent condition in the same manner as those in Figures 11A and D. Figures 11B, E and H show the tangential velocity profiles of the movements recorded in the three blocks illustrated in Figures 11A, D and G. Although one block consisted of 50 trials, only every other (25) trajectory and velocity profile are shown for clarity. The terminal points of these trajectories and velocity profiles correspond to the end of the first ballistic movement. Therefore, neither trajectories nor velocity profiles of movements occurring after the end of the ballistic movement are shown. The trajectories are approximately straight, and the velocity profiles are single-peaked and bell-shaped.

These kinematic features coincide with those of ballistic and pre-planned movements described by other investigators (Abend, Bizzi, & Morasso, 1982; Atkeson & Hollerbach, 1985; Flash & Hogan, 1985; Morasso, 1981; Uno, Kawato, & Suzuki, 1989). Thus, the fundamental kinematic features of the movements in the first block and those in the last block are similar to each other. The movements in the last block, however, become more accurate than those in the first block as shown in Figures 11C and F, which illustrate the original trajectories (Figs. 11A and D) after normalization such that the center of the starting zone and the target of each trial become (0, 0) and (0, 100), respectively.

The end points of the trajectories were distributed over a wide region and most of them undershot the target in the first block, while they concentrated near the target (Figs. 11C and F) in the last block of the first stage. However, the end points were also distributed over a wide region in the first block of the second stage (Fig. 11I), and this suggested that intermanual transfer did not occur under the extrinsically-consistent condition.

-----

Insert Figure 11 about here

-----

### Aiming Error

In Figure 12, the mean and standard error of the aiming error in each block of trials are plotted separately for one of the participants in the extrinsically-consistent group (M.N.) and one in the intrinsically-consistent group (M.Y.). The mean aiming error ( $y$ ) decreased with increasing number of trial blocks ( $x$ ) in both the first and second stages, and was well-fit ( $r > .85$ ) by the exponential decay function:

$$y = k_0 + k_1 e^{-k_2 x} \quad (13)$$

by adjusting the parameters  $k_0$ ,  $k_1$ , and  $k_2$  to minimize the  $\chi^2$  value (Fig. 12).

Furthermore, a one-way analysis of variance (ANOVA) of the mean aiming error with the number of trial blocks as a factor revealed that the number of trial blocks was a significant factor (the first stage of participant M.N.:  $F(11, 586) = 7.38$ ,  $p < .001$ ; the second stage of participant M.N.:  $F(11, 586) = 7.38$ ,  $p < .001$ ; the first stage of participant M.Y.:  $F(11, 588) = 10.28$ ,  $p < .001$ ; the second stage of participant M.Y.:  $F(11, 587) = 12.07$ ,  $p < .001$ ). Post hoc comparisons (Tukey HSD multiple comparisons) between the trial blocks revealed a significant difference in the mean aiming error in the first block versus the last block in all cases ( $p < .001$  level). These results suggest that learning occurred in all stages.

-----

Insert Figure 12 about here

-----

The mean aiming error in the first stage was compared to that in the second stage (Fig. 12) to investigate the difficulty of the aiming task in each of the stages. For the participant (M.N.) in the extrinsically-consistent group, the mean error in the second stage ( $M = 63.11$ ,  $SD = 43.16$ ) was significantly larger than that in the first stage ( $M = 45.05$ ,

$\underline{SD} = 38.09$ ;  $t(1197) = 7.68$ ,  $p < .0001$ ). This result suggests that the aiming task in the second stage was more difficult than that in the first stage. Furthermore, for the participant in the intrinsically-consistent group (M.Y.), the error in the second stage ( $\underline{M} = 38.70$ ,  $\underline{SD} = 30.83$ ) was significantly smaller than that of the first stage ( $\underline{M} = 54.04$ ,  $\underline{SD} = 36.89$ ;  $t(1161) = 7.68$ ,  $p < .0001$ ). Thus, it is unlikely that the reason for the larger aiming error in the second stage was that M.N. was fatigued.

The results of the remaining six participants were similar to those of M.N. or M.Y. (Fig. 13). The mean aiming error in the second stage was significantly larger than that in the first stage for the extrinsically-consistent group, whereas it was significantly smaller for the intrinsically-consistent group. Because M.N. used the right (preferred) arm in the first stage and the left (non-preferred) arm in the second stage, the reason for the larger error in the second stage may be that M.N. (Fig. 12A) used the non-preferred arm. Note that the results of S.M. and H.W., however, who used the left (non-preferred) arm in the first stage and the right (preferred) arm in the second stage, were similar to that of M.N. Therefore, the larger error in the second stage for M.N. did not appear to be due to arm preference.

-----  
 Insert Figure 13 about here  
 -----

### The Effect of Distortion Caused by the Transformation

Table II shows the values of  $b$  (the effect of average velocity on the aiming error) and  $K$  (constant error) estimated from linear regression analysis of the aiming error under normal conditions. The values of  $b$  are significant ( $p < .05$ ) in the majority of cases (14 of 16 cases) and support Schmidt's law.

-----  
 Insert Table II about here  
 -----

The values of the distortion effect ( $a$ ) were estimated from linear regression analysis of the aiming error pooled for each trial block ( $n = 50$  except for some blocks containing the missing trials) using the values of  $b$  and  $K$  shown in Table II. Figure 14 shows the estimated values of  $a$  plotted as a function of the number of trial blocks separately for each of the participants. The majority of values were significant ( $p < .05$ ). For the extrinsically-consistent group, the 99% confidence interval<sup>4</sup> of the estimated value in the last block of the first stage did not overlap that in the first block of the second stage, suggesting that the learning curves of the two stages were discontinuous. For the intrinsically-consistent group, however, the former confidence interval overlapped the latter except in one case (participant Y.F.), suggesting that the learning curves were continuous. Thus, positive intermanual transfer in learning was observed in the intrinsically-consistent group, but no positive transfer was observed in the extrinsically-consistent group.

-----  
 Insert Figure 14 about here  
 -----

## Discussion

To investigate whether the intrinsic kinematics is adaptively represented in the CNS in the control of arm movements, visual feedback during an aiming task was altered by a real-time transform function based on the magnification of the elbow- and shoulder-

joint angles of the participants. A linear transformation of joint angles (intrinsic coordinates) corresponded to a nonlinear transformation of hand and screen coordinates (extrinsic coordinates).

The present study examined whether the participants learned to adjust for a transformation of joint angles in intrinsic coordinates or in extrinsic coordinates, by investigating whether positive intermanual transfer occurred under the extrinsically-consistent condition or intrinsically-consistent condition. The participants practiced the aiming task under a linear transformation of the joint angles in the first stage of both conditions. On the one hand, when the participants executed the aiming task under the same mapping between the screen and the hand coordinates using the different arm in the succeeding stage (extrinsically-consistent condition), no positive intermanual transfer was observed, that is, 1) the aiming error in the second stage was larger than that in the first stage, and 2) the learning curves of the two stages were discontinuous. On the other hand, when the participants executed the aiming task under the same transformation of the joint angles using the different arm in the succeeding stage (intrinsically-consistent condition), positive intermanual transfer was observed, that is, 1) the aiming error in the second stage was smaller than that in the first stage, and 2) the learning curves of the two stages were continuous. The results suggest that the participants learned to adjust for the transformation in the first stage in intrinsic coordinates.

The fact that positive intermanual transfer of learning was observed under the intrinsically-consistent condition suggests that adjustments were made to a central representation not specific to either arm but common to both arms. This result is at least partly consistent with previous physiological findings. Tanji, Okano, and Sato (1987) reported that the firing rates of primary motor cortex neurons are directly correlated with contralateral muscle activity. The majority of non-primary motor cortices, such as the supplementary motor cortex and the pre-motor cortex, however, do not appear to code the

activity of particular muscles, because their discharge rates are independent of the hand used (i.e., their firing rates increased when the monkey used the right hand or the left hand). Rather, these neurons appear to encode the particular motor task (in this case "pressing a button"). These physiological findings, indicate that there are two functional levels in motor control systems, one level is hand- (or muscle-) specific and the other is non-specific. Presently, however, there are little data concerning the neurological locus or correlates of motor learning specific to either arm or both arms.

One possible reason why the aiming error was larger in the second stage under the extrinsically-consistent condition compared to that in the first stage is as follows. The mapping between the hand and screen coordinates used in the second stage under the extrinsically-consistent condition was very complicated and nonlinear as represented by Equation 5 while the transform in the first stage was simply represented as Equation 2. Although there is no assurance that the mathematical complexity and nonlinearity correspond to the difficulty of learning for a biological system, it appears that the transformation by Equation 5 is more difficult in the CNS than the simple magnifications of joint angles represented by Equation 2. However, it is unclear whether the participants learned the transformation used in the second stage under the extrinsically-consistent condition in intrinsic coordinates. There is a possibility that the participants adjusted to the transformation in the first stage in terms of intrinsic coordinates and adjusted to the transformation in the second stage in terms of extrinsic coordinates. One participant of the extrinsically-consistent group (M.N.) reported that he tried to remember the relation between the hand and the screen planes in the later blocks in the second stage.

In any case, the fact that positive intermanual transfer could not be observed under the extrinsically-consistent condition implies that the participants tried to adjust for the different transformations in the intrinsic coordinates or that they tried to adjust for the transformations in coordinates that differed in the first stage from the second stage.

It is still unclear whether the participants learned to adjust to the transformation of joint angles in terms of kinematic parameters or dynamic parameters (e.g., joint torque and muscle tension). It appears unlikely, however, that the participants learned it in terms of dynamic parameters, because the relation between the intrinsic kinematic coordinate variables and the intrinsic dynamic coordinate variables is highly nonlinear. A linear transform of joint angles becomes nonlinear and complex when represented in dynamic parameters. In other words, when the shoulder- and elbow-joint angles are multiplied by  $\dot{\theta}$  and  $\ddot{\theta}$ , respectively, the inertial and viscous forces of the shoulder joint increase approximately in proportion to  $\dot{\theta}$ , the centripetal and Coriolis forces increase approximately in proportion to  $\dot{\theta}^2$  and  $\dot{\theta}$ , respectively, the elastic force is constant, and the resultant joint torque is the sum of these forces. Furthermore, this nonlinear and complex transform of joint torques is unlikely to become linear and simple when it is represented as other dynamic parameters that the biological motor system may use (e.g., muscle tension and motor neuron activity). Thus, it appears reasonable to assume that the participants learned to adjust to the transformation of joint angles in terms of kinematic parameters.

Recent behavioral and neurophysiological studies have suggested how the intrinsic kinematics is used in the CNS to control arm movements. Some of them indicate that the intrinsic kinematics is used to represent the target's locations and others indicate that it is used to represent the motion trajectories. Soechting and Flanders (1989a, 1989b) investigated pointing errors in a three-dimensional space and showed that they can account for the observed errors on assumption that the CNS does not directly compute the muscle tensions from the visual information of the target's locations relative to the shoulder but that it computes the shoulder and the elbow joint angles from the target's locations. Graziano, Yap, and Gross (1994) found that the position of the visual receptive field of neurons in the premotor cortex of monkeys changes as the intrinsic kinematic information

changes (i.e., hand position represented by joint angle or muscle length). They showed that these neurons respond to visual stimuli and that the visual receptive field includes areas that surround sections of the surface of the body, such as the hand or arm. Furthermore, the visual receptive field moves with the arm, even when the arm is passively moved without visual feedback. These studies suggest that the intrinsic kinematics is closely related to the visual information of the target locations.

Kalaska and his colleagues suggested that a trajectory is represented in terms of intrinsic kinematics by neuronal activity in area 5 in monkeys. As mentioned in the Introduction, area 5 neurons encode the intrinsic kinematics of arm movements (Kalaska, Cohen, Prud'homme, & Hyde 1990; Lacquaniti, Guigon, Bianchi, Ferraina, & Caminiti, in press). Kalaska et al. (1990) reported that some of the directionally-tuned cells in area 5 exhibit marked changes in discharge prior to reaching movements. The time function of their discharge rate closely resembles that of the movement velocity (i.e., a bell-shaped function). This suggests that the activity of these phasic cells encodes a time sequence of movement velocities along the path. Rosenbaum and his colleagues (e.g., Rosenbaum, Loukopoulos, Meulenbroek, Vaughan & Engelbrecht, 1995) proposed a kinematic model of motion control (Knowledge model) in which postures are stored as vectors in joint space and used to select reaching movements evaluating accuracy costs and travel costs.

In conclusion, the results of the present study suggest that a representation of intrinsic kinematics is formed in the CNS and used in the control of reaching movements during the learning of an aiming task. Moreover, this representation appears to be continuously adaptive, able to adjust in response to novel circumstances. The presence of an adaptive representation corresponding to the intrinsic kinematics in the CNS supports the hierarchical model rather than the non-hierarchical model of visually-guided reaching movements.



where,  $\theta_1^*$  and  $\theta_2^*$  are the joint angles after the transformation,  $k_1$  and  $k_2$  are magnification or minimization factors, and  $h_1$  and  $h_2$  are constant values. The transformation of joint angles of the other arm configuration  $(\theta_1, \theta_2)$  in the same manner as Equation 15 gives

$$\begin{aligned}\theta_1^* &= k_1 \theta_1 + h_1 \\ \theta_2^* &= k_2 \theta_2 + h_2.\end{aligned}\quad (16)$$

The transformed joint angles  $(\theta_1^*, \theta_2^*)$  can be represented by those of the actual arm configuration  $(\theta_1, \theta_2)$  using the same relation as Equation 7:

$$\begin{aligned}\theta_1^* &= \theta_1 - 2\arctan \frac{l_2 \sin \theta_2^*}{l_1 + l_2 \cos \theta_2^*} \\ \theta_2^* &= \theta_2.\end{aligned}\quad (17)$$

Substituting Equation 7 into Equation 16 and then substituting Equation 16 into Equation 17 gives

$$\begin{aligned}\theta_1^* &= k_1 \theta_1 + (1 - k_1) \left[ \theta_1 - 2\arctan \frac{l_2 \sin \theta_2}{l_1 + l_2 \cos \theta_2} \right] + h_1 \\ &\quad - 2\arctan \frac{l_2 \sin(k_2 \theta_2 + h_2)}{l_1 + l_2 \cos(k_2 \theta_2 + h_2)} \\ \theta_2^* &= k_2 \theta_2 + h_2.\end{aligned}\quad (18)$$

Thus, Equation 5 is obtained by replacing  $k_1$  and  $k_2$  with 1.25 and 0.5, respectively.

## Appendix B

### Additional Experiment to Test the Effect of a Slightly Different Ratio of the Marker Movement to the Cursor Movement

An experiment was conducted to test the effect of different ratios of the marker movement to the cursor movement in the  $x$  and  $y$  directions. The aiming error was compared when the ratios in the  $x$  and  $y$  directions were identical (1.0:1.0 in both directions) to that when the ratios were different (1.0:1.0 in the  $x$  direction and 1.0:0.8 in the  $y$  direction).

#### Methods

Participants. Three volunteers who did not participate in the main experiment participated in this experiment. All participants were naive as to the purpose of this experiment and self-reported to be right-handed.

Apparatus and procedure. The apparatus was the same as that used in the main experiment, and the procedure was similar. Visual feedback was not altered in this experiment. There were two types of trials: identical and different trials. In the identical trials, the ratios in the  $x$  and  $y$  directions of the marker movement to the cursor movement were identical (1.0:1.0 in both directions). In the different trials, they were different (1.0:1.0 in the  $x$  direction and 1.0:0.8 in the  $y$  direction).

The participants completed two blocks of 50 trials. The two types of trials were randomly mixed within a block so that the total number of each type was 25. A 3 min rest period was allowed between blocks. The participants were not informed of the two types of trials nor of the ratio of the marker movement to the cursor movement.

## Results and Discussion

Table B1 shows the mean and standard deviation of the aiming error in the identical trials and different trials. A  $t$ -test with 98  $df$  was performed separately for the data from each participant. There was no significant difference between the two types of trials. Additionally, none of the participants realized that different types of trials existed. The results suggest that the slight difference of the ratio did not significantly affect the aiming error. Therefore, the data of the participants (H.W., M.N., Y.F., and M.Y.), who conducted the aiming task with different ratios in the main experiment, was analyzed in the same manner as that of the other participants.

-----  
Insert Table B1 about here  
-----

## References

- Abend, W., Bizzi, E., & Morasso, P. (1982). Human arm trajectory formation. Brain, *105*, 331-348.
- Alexander, G. E., DeLong, M. R., & Crutcher, M. D. (1992). Do cortical and basal ganglionic motor areas use "motor programs" to control movement? Behavioral and Brain Sciences, *15*, 656-665.
- Atkeson, C. G. (1989). Learning arm kinematics and dynamics. Annual Review of Neuroscience, *12*, 157-183.
- Atkeson, C. G. & Hollerbach, J. M. (1985). Kinematic features of unrestrained vertical arm movements. Journal of Neuroscience, *5*, 2318-2330.
- Bedford, F. L. (1989). Constraints on learning new mappings between perceptual dimensions. Journal of Experimental Psychology: Human Perception and Performance, *15*, 232-248.
- Cook, T. W. (1933). Studies in cross education. I. Mirror tracing the star-shaped maze. Journal of Experimental Psychology, *16*, 145-160.
- Cunningham, H. (1989). Aiming error under transformed spatial mappings suggests a structure for visual-motor maps. Journal of Experimental Psychology: Human Perception and Performance, *15*, 493-506.
- Flash, T. & Hogan, N. (1985). The coordination of arm movements: An experimentally confirmed mathematical model. The Journal of Neuroscience, *5*, 1688-1703.
- Flowers, K. (1975). Ballistic and corrective movements on an aiming task: Intention tremor and parkinsonian disorders compared. Neurology, *25*, 413-421.
- Graziano, M. S. A., Yap, G. S., & Gross, C. G. (1994). Coding of visual space by premotor neurons. Science, *266*, 1054-1057.

- Held, R. & Gottlieb, N. (1958). Technique for studying adaptation to disarranged hand-eye coordination. Perceptual and Motor Skills, 8, 83-86.
- Held, R. & Hein, A. V. (1958). Adaptation of disarranged hand-eye coordination contingent upon re-afferent stimulation. Perceptual and Motor Skills, 8, 87-90.
- Hollerbach, J. M. (1982). Computers, brains and the control of movement. Trends in Neurosciences, 5, 189-192.
- Hollerbach, J. M. (1990). Fundamentals of motor behavior. In D. N. Osherson, et al. (Eds.), Visual cognition and action Vol. 2, (pp. 153-182). Cambridge, Mass: MIT Press.
- Imamizu, H. & Shimojo, S. (1995). The locus of visual-motor learning at the task or manipulator level: Implications from intermanual transfer. Journal of Experimental Psychology: Human Perception and Performance, 21, 719-733.
- Kalaska, J. F., Caminiti, R., & Georgopoulos, A. P. (1983). Cortical mechanisms related to the direction of two dimensional arm movements: Relations in parietal area 5 and comparison with motor cortex. Experimental Brain Research, 51, 247-260.
- Kalaska, J. F., Cohen, D. A. D., Prud'homme, M., & Hyde, M. L. (1990). Parietal area 5 neuronal activity encodes movement kinematics, not movement dynamics. Experimental Brain Research, 80, 351-364.
- Kalaska, J. F. & Crammond, D. J. (1992). Cerebral cortical mechanisms of reaching movements. Science, 255, 1517-1523.
- Lacquaniti, F., Guigon, E., Bianchi, L., Ferraina, S., & Caminiti, R. (in press). Representing spatial information for limb movement: Role of area 5 in the monkey. Cerebral Cortex.
- Massone, L. & Bizzi, E. (1989). A neural network model for limb trajectory formation. Biological Cybernetics, 61, 417-425.

- Milner, B., Corkin, S., & Teuber, H. L. (1968). Further analysis of the hippocampal amnesic syndrome: 14-year follow-up study of H. M. Neuropsychologia, *6*, 215-234.
- Morasso, P. (1981). Spatial control of arm movements. Experimental Brain Research, *42*, 223-227.
- Pollick, F. E. & Ishimura, G. (1996). The three-dimensional curvature of straight-ahead movements. Journal of Motor Behavior, *28*, 271-279
- Rosenbaum, D. A. (1991) Human motor control. New York: Academic Press.
- Rosenbaum, D. A., Loukopoulos, L. D., Meulenbroek, R. G., Vaughan, J. & Engelbrecht, S. E. (1995) Planning reaches by evaluating stored postures. Psychological Review, *102*, 28-67.
- Saltzman, E. (1979). Levels of sensorimotor representation. Journal of Mathematical Psychology, *20*, 91-163.
- Saltzman, E. & Kelso, J. A. S. (1987). Skilled actions: A task-dynamic approach. Psychological Review, *94*, 84-106.
- Schmidt, R. A., Zelaznik, H., Hawkins, B., Frank, J. S., & Quinn, J.T. (1979). Motor output variability: A theory for the accuracy of rapid motor acts. Psychological Review, *86*, 415-451.
- Soechting, J. F. & Flanders, M. (1989a) Sensorimotor representations for pointing to targets in three dimensional space. Journal of Neurophysiology, *62*, 582-594.
- Soechting, J. F. & Flanders, M. (1989b) Errors in pointing are due to approximations in sensorimotor transformations. Journal of Neurophysiology, *62*, 595-608.
- Tanji, J., Okano, K., & Sato, K. C. (1987). Relation of neurons in the nonprimary motor cortex to bilateral hand movement, Nature, *327*, 618-620.
- Uno, Y., Kawato, M., & Suzuki, R. (1989). Formation and control of optimal trajectory in human arm movement: Minimum torque-change model. Biological Cybernetics, *61*, 89-101.

Welch, R. B. (1978). Perceptual modification. New York: Academic Press.

Woodworth, R. S. (1899). The accuracy of voluntary movement. Psychological Review  
Monograph (Suppl.) 3: Cited in Flowers (1975)

### Author Notes

Hiroshi Imamizu, Yoji Uno, and Mitsuo Kawato, Advanced Telecommunications Research (ATR) Human Information Processing Research Laboratories, Kyoto, Japan.

Hiroshi Imamizu is now a member of the Kawato Dynamic Brain Project, Japan Science and Technology Corporation, Kyoto, Japan. Yoji Uno is now at the Department of Information and Computer Sciences, Toyohashi University of Technology, Aichi, Japan.

We are grateful to Frank E. Pollick for developing the method of detecting the end point of the first ballistic movement. We thank Carol A. Fowler and Helen Cunningham for their helpful suggestions.

Correspondence concerning this article should be addressed to Hiroshi Imamizu, Kawato Dynamic Brain Project, Japan Science and Technology Corporation, 2-2 Hikaridai, Seika-cho, Soraku-gun, Kyoto, 619-02, Japan. Electronic mail may be sent via the Internet to [imamizu@erato.atr.co.jp](mailto:imamizu@erato.atr.co.jp).

## Footnotes

1 For four participants (H.W., M.N., Y.F., and M.Y.), the ratio in the  $x$  direction (1.0 : 1.0) was slightly different from that in the  $y$  direction (1.0 : 0.8, see Figure 5 for the definitions of the directions) due to an incorrect setting of the CRT monitor. The ratio in the  $x$  direction was equal to that in the  $y$  direction (1.0 : 1.0) for the other participants. Therefore, an additional experiment was conducted to test the effect of the different ratios (see Appendix B). The results of this experiment clearly showed that the ratio difference did not significantly affect the aiming error. Consequently, the data of the four participants were analyzed using the same methods as that for the other participants.

2 Woodworth (1899) made a distinction between the components for voluntary movements in the aiming task: an initial impulse phase and a series of secondary adjustments made subsequently to attain the final target position. The first component is a fast, preprogrammed ballistic movement that brings the hand into the general area of the target. The second component comprises a number of adjustments. In this latter phase, movements are continuously monitored and adjusted in relation to sensory information. The first component, the initial impulse phase in Woodworth's terminology, can be called a ballistic movement and the second current control component can be called a corrective movement (Flowers, 1975).

3 A Welch test was used instead of a  $t$ -test when the variances of the two groups could not be considered to be equal to each other, that is, the  $F$  ratio of one group to the other was significantly large ( $p < .05$ ).

4 In the linear regression analysis, the  $100(1 - \alpha)\%$  confidence interval of the estimated value ( $\hat{\beta}$ ) is defined as

$$\hat{\beta} - t(\alpha/2, n - p) SE \quad \hat{\beta} + t(\alpha/2, n - p) SE ,$$

where  $n$  is the number of data,  $p$  is the number of parameters in the assumed linear model,  $t(\alpha/2, n - p)$  is the upper  $100(1 - \alpha/2)\%$  point of the  $t$ -distribution, and  $SE$  is the standard error of the estimated value.

Table I Learning schedule of each participant

Group	Participants	Arm used	Arm used
		in the first stage	in the second stage
Extrinsically- consistent	H.W. and S.M.	Left	Right
	M.N. and K.S.	Right	Left
Intrinsically- consistent	Y.F. and Y.H.	Left	Right
	M.Y. and K.A	Right	Left

**Table II.** Estimated values of  $b$  and  $K$  from the aiming error under normal conditions.

Participant	Right Arm		Left Arm	
	$b$ (mm)	$K$ (mm)	$b$ (mm)	$K$ (mm)
H.W.	12.73 <sup>n.s.</sup>	16.64 <sup>***</sup>	25.80 <sup>***</sup>	10.10 <sup>**</sup>
S.M.	12.56 <sup>*</sup>	12.92 <sup>***</sup>	37.84 <sup>***</sup>	2.27 <sup>n.s.</sup>
M.N.	55.65 <sup>***</sup>	-3.57 <sup>n.s.</sup>	55.65 <sup>***</sup>	10.66 <sup>***</sup>
K.S.	47.08 <sup>***</sup>	-3.57 <sup>n.s.</sup>	73.99 <sup>***</sup>	-10.12 <sup>*</sup>
Y.F.	45.31 <sup>***</sup>	3.66 <sup>n.s.</sup>	13.93 <sup>n.s.</sup>	19.71 <sup>***</sup>
Y.H.	18.84 <sup>*</sup>	16.62 <sup>***</sup>	62.54 <sup>***</sup>	0.29 <sup>n.s.</sup>
M.Y.	44.31 <sup>***</sup>	7.75 <sup>n.s.</sup>	27.35 <sup>**</sup>	14.50 <sup>**</sup>
K.A.	28.21 <sup>***</sup>	10.08 <sup>**</sup>	18.87 <sup>***</sup>	10.09 <sup>**</sup>

**Note.** <sup>n.s.</sup> Not significant; \*  $p < .05$ ; \*\*  $p < .01$ ; \*\*\*  $p < .001$ ;

$b$  and  $K$  are defined in Equation 12.

Table B1. Means and standard deviations of the aiming error for identical and different trials for each participant.

Participant	Identical		Different		t-value	probability
	<u>M</u>	<u>SD</u>	<u>M</u>	<u>SD</u>		
R.O.	24.53	12.12	23.97	11.29	0.04	.83
T.F.	34.09	18.16	28.90	17.74	2.09	.15
T.Y.	36.98	21.62	37.72	20.95	0.03	.86

Note. Units of the mean (M) and the standard deviation (SD) are in mm.

## Figure Captions

Figure 1 Schematic diagram of visual-motor control based on a hierarchical approach. The top row illustrates the computational modules and the intermediate representations connecting each module. The next two rows illustrate examples of representations in robot control.  $(x, y)$  denotes the Cartesian coordinates of the object's position.  $\theta_1$  and  $\theta_2$  denote the shoulder-joint angle and elbow-joint angle, and  $\tau_1$  and  $\tau_2$  denote the shoulder-joint torque and elbow-joint torque. Paths in the joint space and in the torque space are arbitrary examples in point-to-point reaching movements.

Figure 2 Schematic diagram of visual-motor control based on a non-hierarchical approach. The computational model is at the top with the neural network model underneath (Massone and Bizzi, 1989).

Figure 3 Overview of the experimental setup illustrated from behind the right shoulder of the participant.

Figure 4 An illustration of the transform in extrinsic coordinates ( $f$ ) in the top figure and that in intrinsic coordinates ( $g$ ) in the bottom figure.  $(x, y)$  denotes the Cartesian coordinates of the hand position with the origin at the shoulder.  $\theta_1$  and  $\theta_2$  denote the shoulder-joint angle and elbow-joint angle. The filled circles indicate the hand positions before the transformation and the open circles indicate those after the transformation.

Figure 5 An illustration of joint angle transformation. The top portion is a front view of the CRT screen, and the bottom is a top view of the participant. The shoulder- and

elbow-joint angles ( $\theta_1$  and  $\theta_2$ , respectively) when the hand is located at a fixed point for this transformation (indicated by a cross), are  $h_1$  and  $h_2$ , respectively.

**Figure 6** Illustrations of the experimental design. The grids in each of the panels show the mapping between the screen coordinates ( $x$ - $y$ : the upper panels) and the hand coordinates ( $p$ - $q$ : the lower panels). As the participant moved the hand along the straight grid lines (the lower panels), the cursor trajectories on the screen became curved lines (the upper panels). The participants learned the same mapping between the screen coordinates and hand coordinates in the first and the second stages under the extrinsically-consistent condition (**A** and **B**) while they learned the same transformation of the joint angles in both stages under the intrinsically-consistent condition (**A** and **C**).  $\theta_1$  and  $\theta_2$  denote the shoulder-joint angle and elbow-joint angle of the actual arm configuration (solid lines) of the participants.  $\theta_1'$  and  $\theta_2'$  denote the joint angles of the other geometrically possible arm configuration (broken lines) whose forearm length, upper arm length and positions of the shoulder and hand were the same as those of the actual arm configuration.

**Figure 7** Predictions of the results under the extrinsically-consistent condition and the intrinsically-consistent condition. **A** Illustration of the prediction of the results on the assumption that the participant learns to adjust for the transformation in the first stage as a nonlinear one in terms of the screen and hand coordinates (i.e., extrinsic coordinates). **B** Illustration of the prediction of the results on the assumption that the participant learns to adjust for the transformation in the first stage as a linear one in terms of the joint angles (i.e., intrinsic coordinates).

**Figure 8** Determination of test area and starting and target positions. **A** Definition of the test area (hatched area); top view of the hand plane. **B** Targets (filled circles) and

starting zones (open circles) in a trial block on the screen (in the screen coordinates). Each pair connects a target and a starting zone (in a trial) by a solid line. The broken lines indicate the border of the screen. These fifty pairs were used in one of the trial blocks for participant K.A. **C** Targets and starting zones on the board (in the hand coordinates) corresponding to those shown in Figure B. The broken lines show the border of the test area.

Figure 9 Detection of the first ballistic movement. **A** and **B** A typical trajectory: panel **A** illustrates the entire trajectory, and panel **B** focuses on the part of it near the target. The open circle and the filled circle indicate the starting zone and the target, respectively. The square indicates the end point of the first ballistic movement. **C** Tangential velocity (solid line) and curvature (gray bars) are plotted against time from the onset of the first auditory cue signaling the beginning of the trial.

Figure 10 Definition of  $V$  indicates the degree of distortion caused by the transformation. **A** and **B** illustrate trajectories of the cursor on the CRT screen and the hand on the board, respectively. These two figures are overlapped in **C**. The vector  $S$  represents the displacement from the starting point on the board to that on the screen, and the vector  $G$  represents the displacement from the target on the board to that on the screen. A scalar  $V$  is defined as the absolute value of subtraction of vector  $S$  from vector  $G$ .

Figure 11 Trajectory and velocity profiles. **A**, **D** and **G** Trajectories of the hand coordinates of one participant (K.S.) in the first and the last trial blocks of the first stage, and in the first trial block of the second stage, respectively. The dots are 10 ms apart (i.e., sampled at 100 Hz).  $(0, 0)$  is a fixed point for the transformation (position of the shoulder of the participant is  $(0, -384)$ ). Every other trajectory (25 each) of the trial blocks is

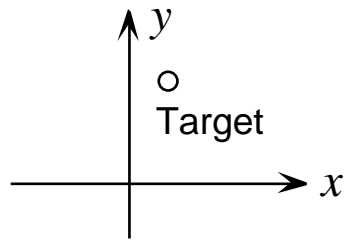
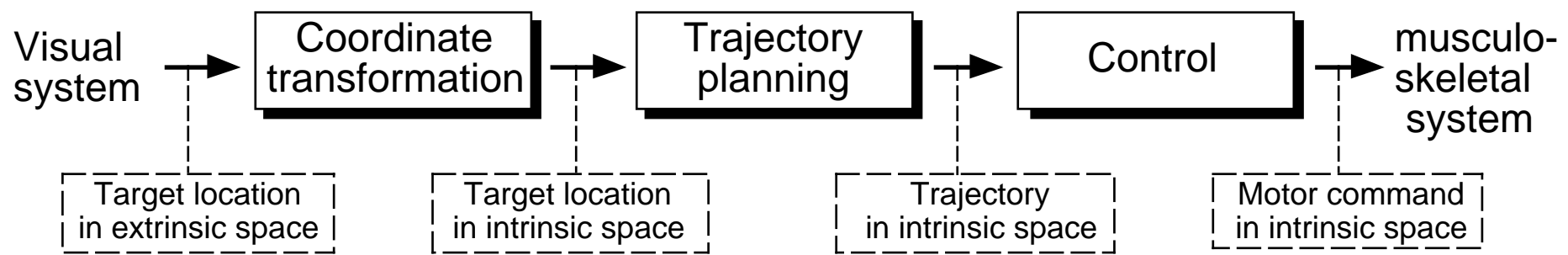
superimposed on each graph. The terminal points of the trajectories correspond to the end of the first ballistic movement. **B**, **E** and **H** Tangential velocity profiles of the trajectories shown in A, D and G, respectively. **C**, **F** and **I** Trajectories that were normalized so that the center of the starting zone and the target of each trial became (0, 0) and (100, 0), respectively. The filled circles indicate the normalized position of the target.

**Figure 12** Aiming error as a function of the number of trial blocks. **A** shows a typical result of a participant in the extrinsically-consistent group (M.N.) while **B** shows that of a participant in the intrinsically-consistent group (M.Y.). The error bars represent the standard error of the mean, and the gray bars indicate the mean aiming error of each stage. The solid lines and equations show the best fitting lines using the least squares method.  $r$  is the correlation coefficient between the mean aiming error and the predicted best fit value.

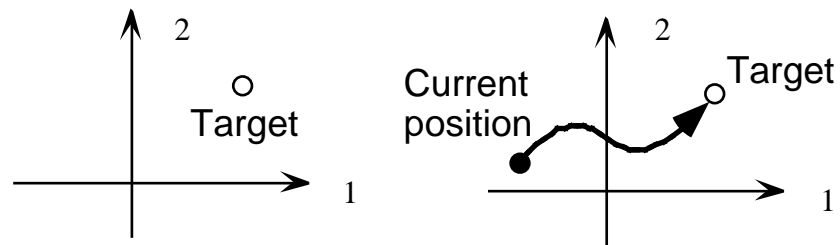
**Figure 13** Aiming error as a function of the number of trial blocks for the participants other than M.N. and M.Y., whose results are shown in Figure 12. The conventions are the same as for Figure 12. (Right) and (Left) indicate the arm that the participant used in each of the stages.

**Figure 14** Effect of distortion caused by the transform on the aiming error as a function of the number of trial blocks. The errors of each trial block were analyzed using linear regression analysis. The open circles, gray filled circles, and black filled circles indicate that the estimated values are significant ( $p < .05$ ), marginal ( $.05 \leq p \leq .1$ ), and not significant ( $p > .1$ ), respectively. The error bars represent 99% confidence intervals, and the gray rectangles highlight the confidence intervals of the last block of the first stage

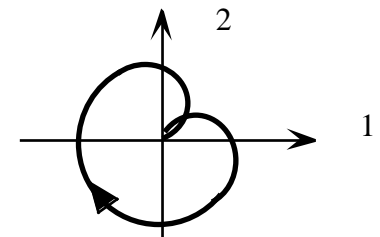
and the first block of the second stage to show continuity or discontinuity of the learning curves. (Right) and (Left) indicate the arm that the participant used in each of the stages.



Extrinsic kinematics



Intrinsic kinematics



Intrinsic dynamics

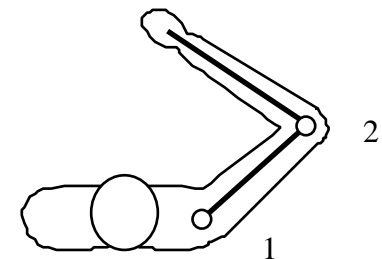
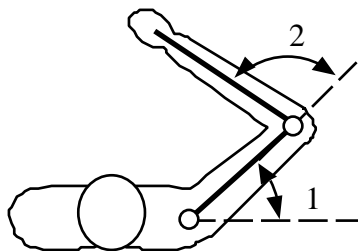
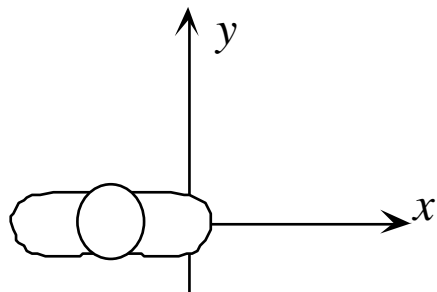


Fig. 1

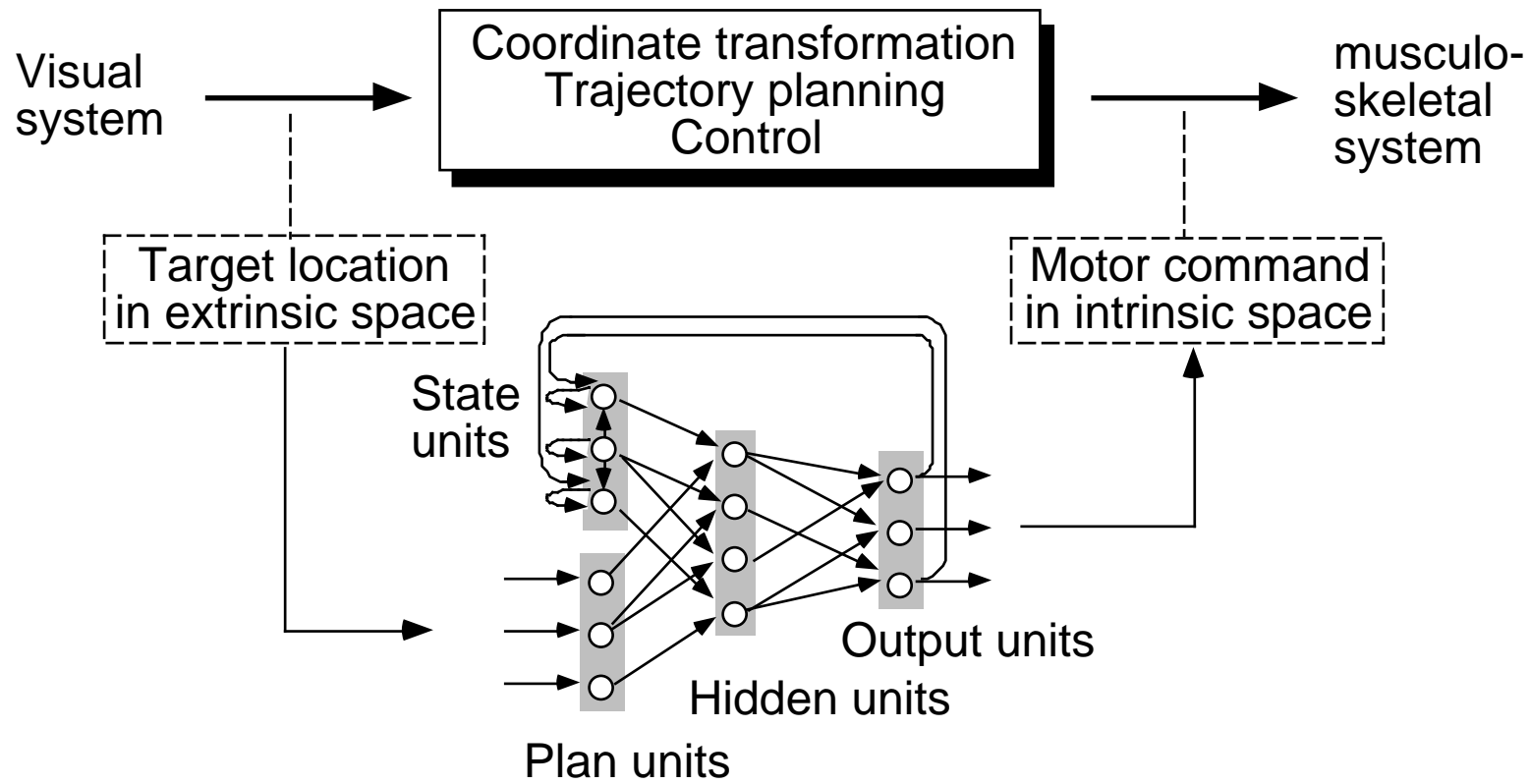
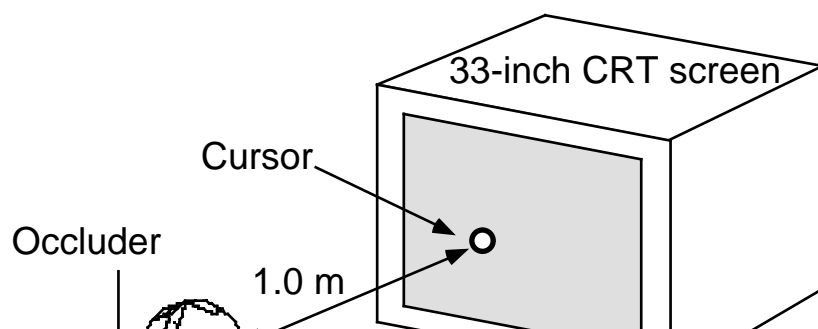


Fig. 2



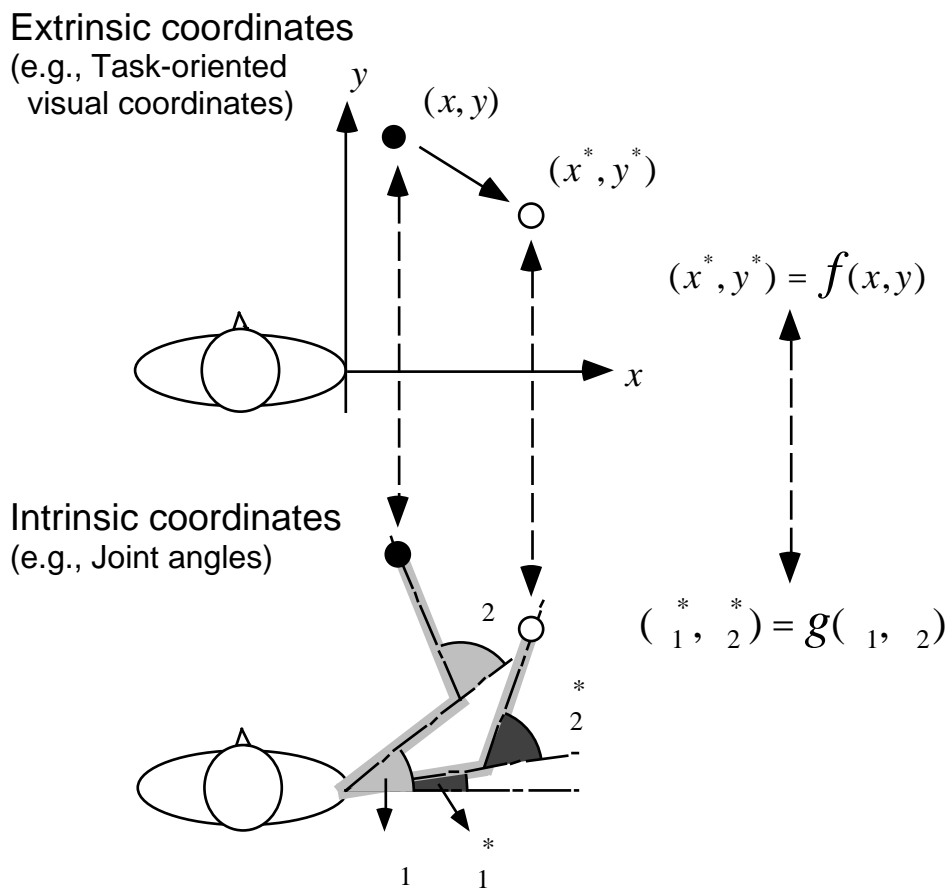


Fig.4

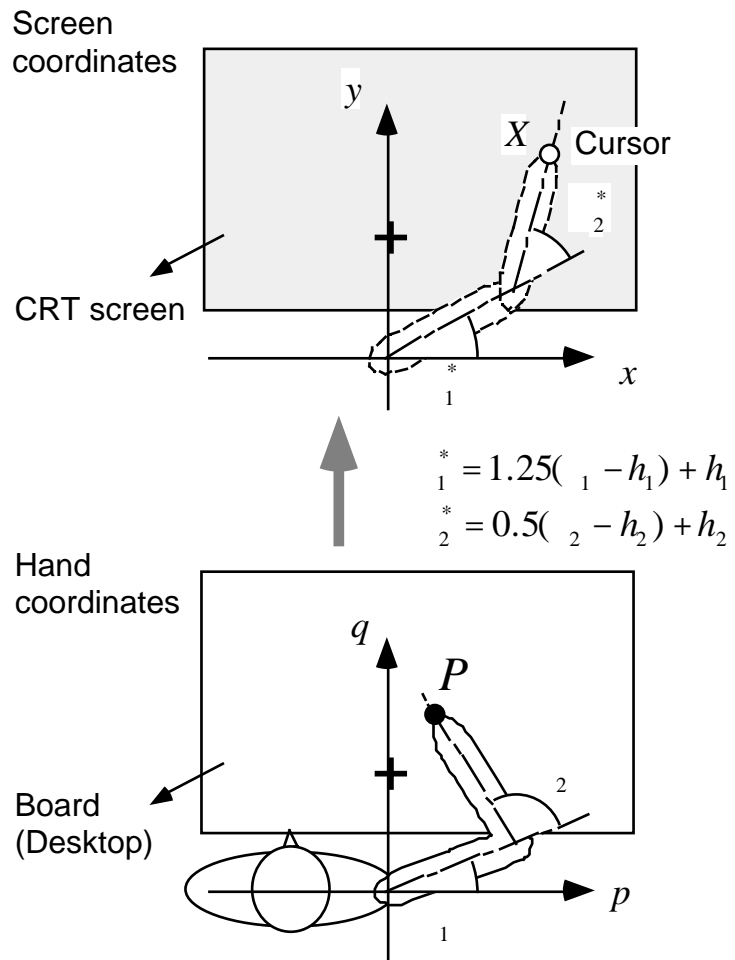


Fig. 5

**A** First stage of any condition

**B** Second stage of extrinsically-consistent condition

**C** Second stage of intrinsically-consistent condition

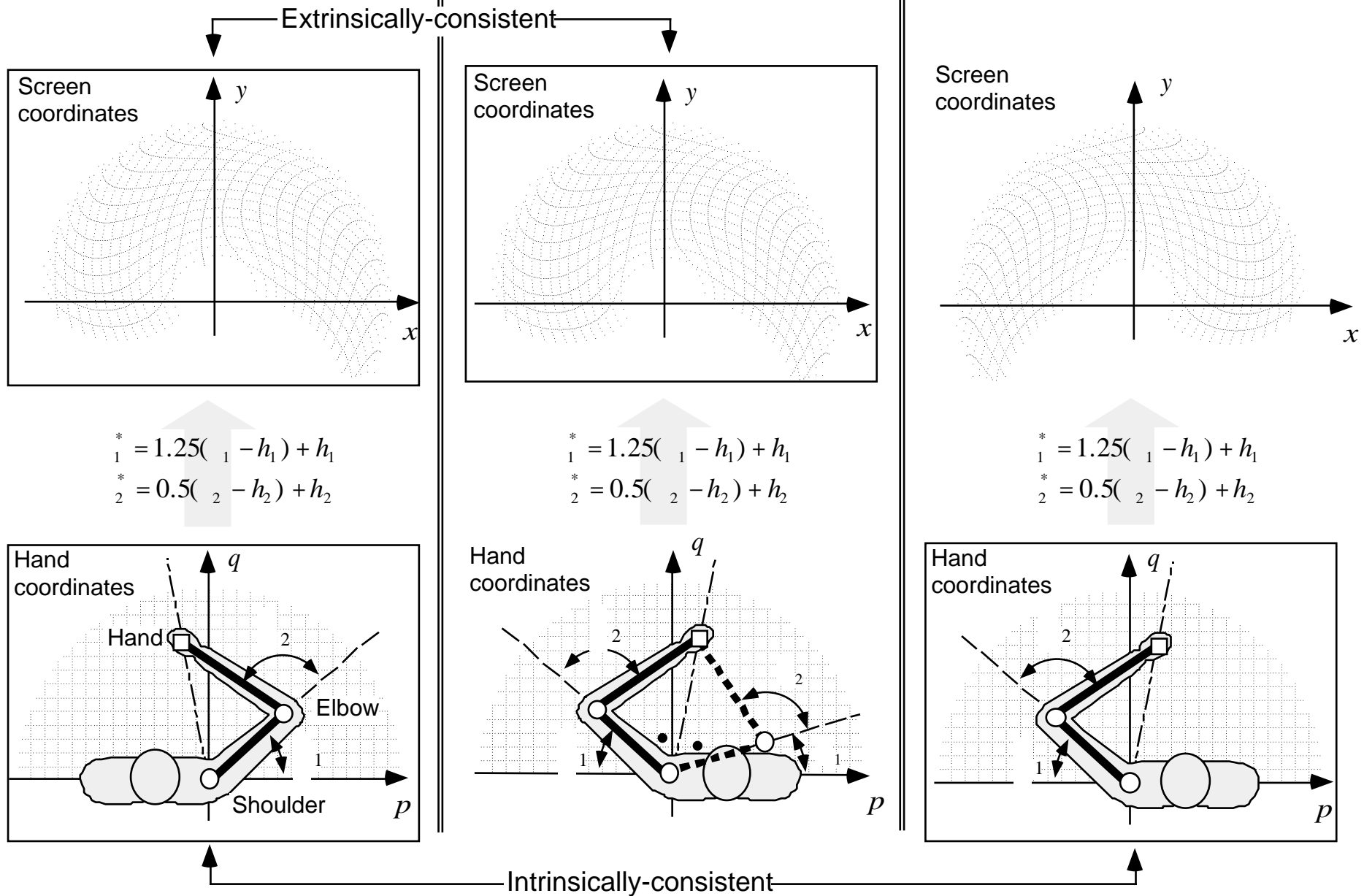


Fig. 6

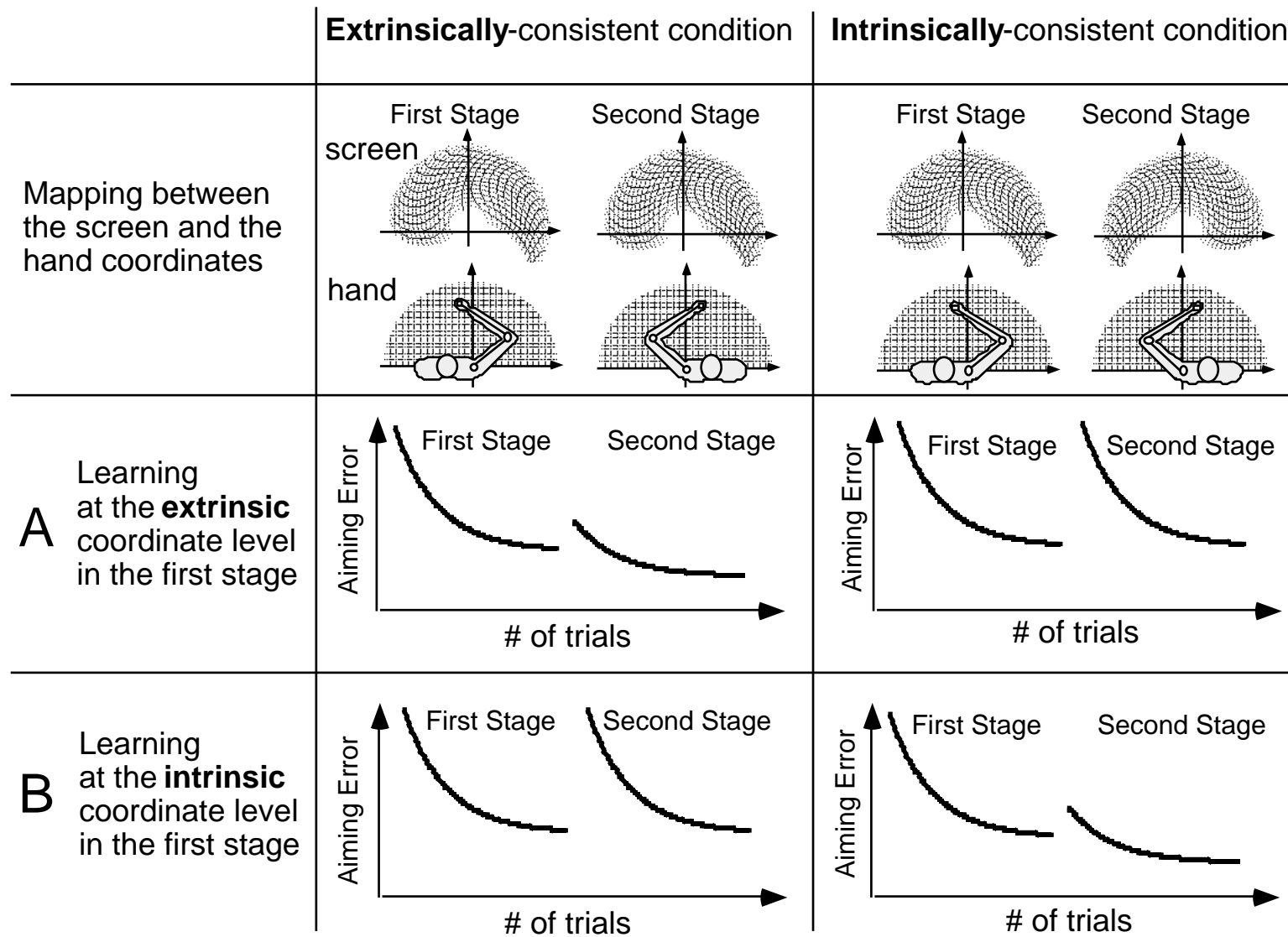


Fig.7



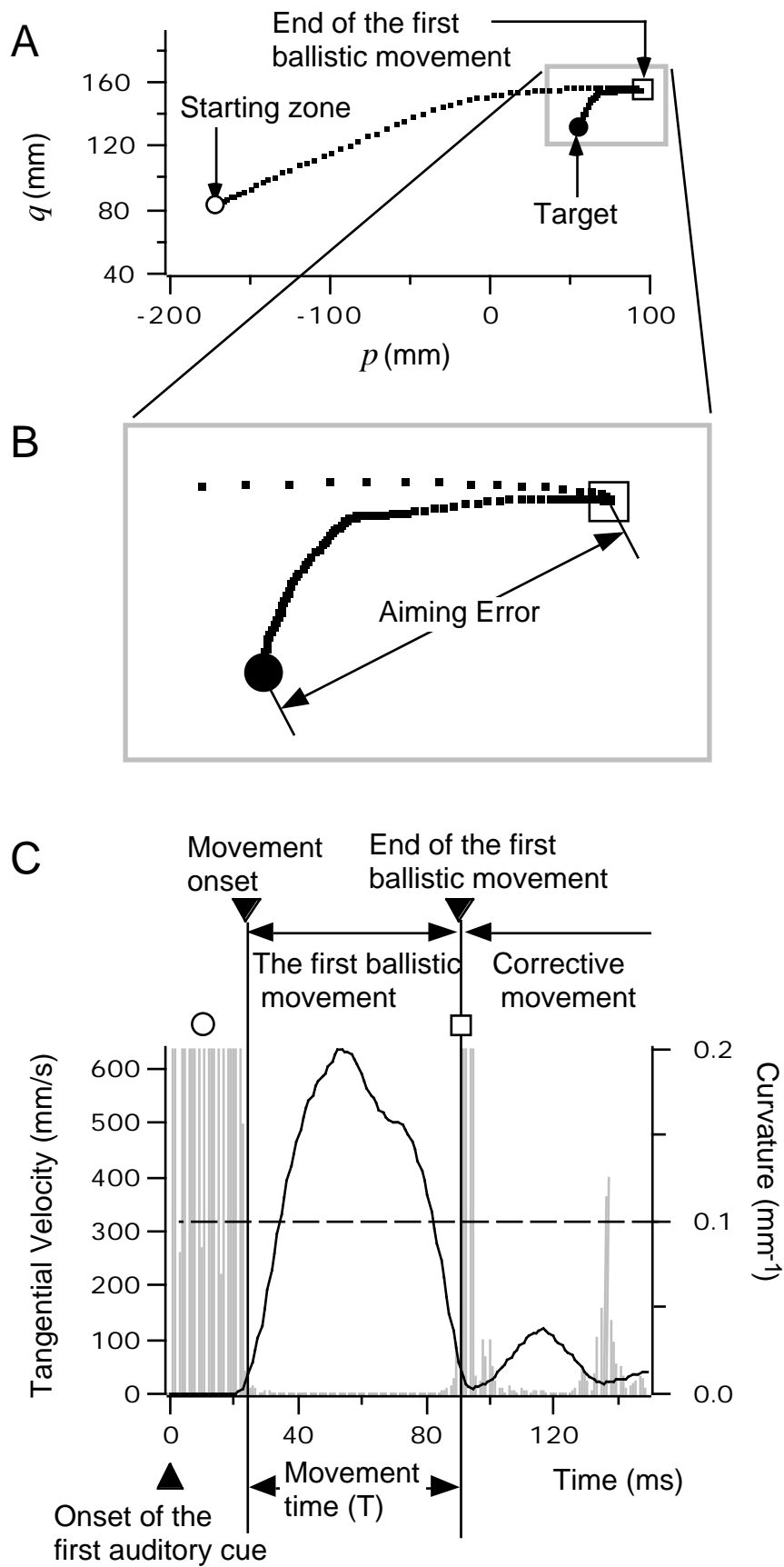
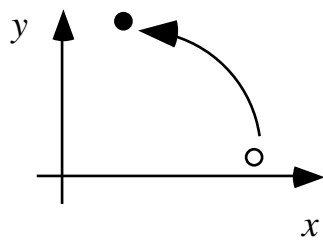
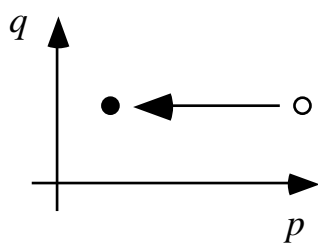


Fig. 9

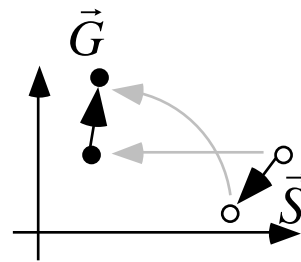
**A** Screen coordinates



**B** Hand coordinates



**C** Overlapped



$$V = |\vec{G} - \vec{S}|$$

*Fig. 10*

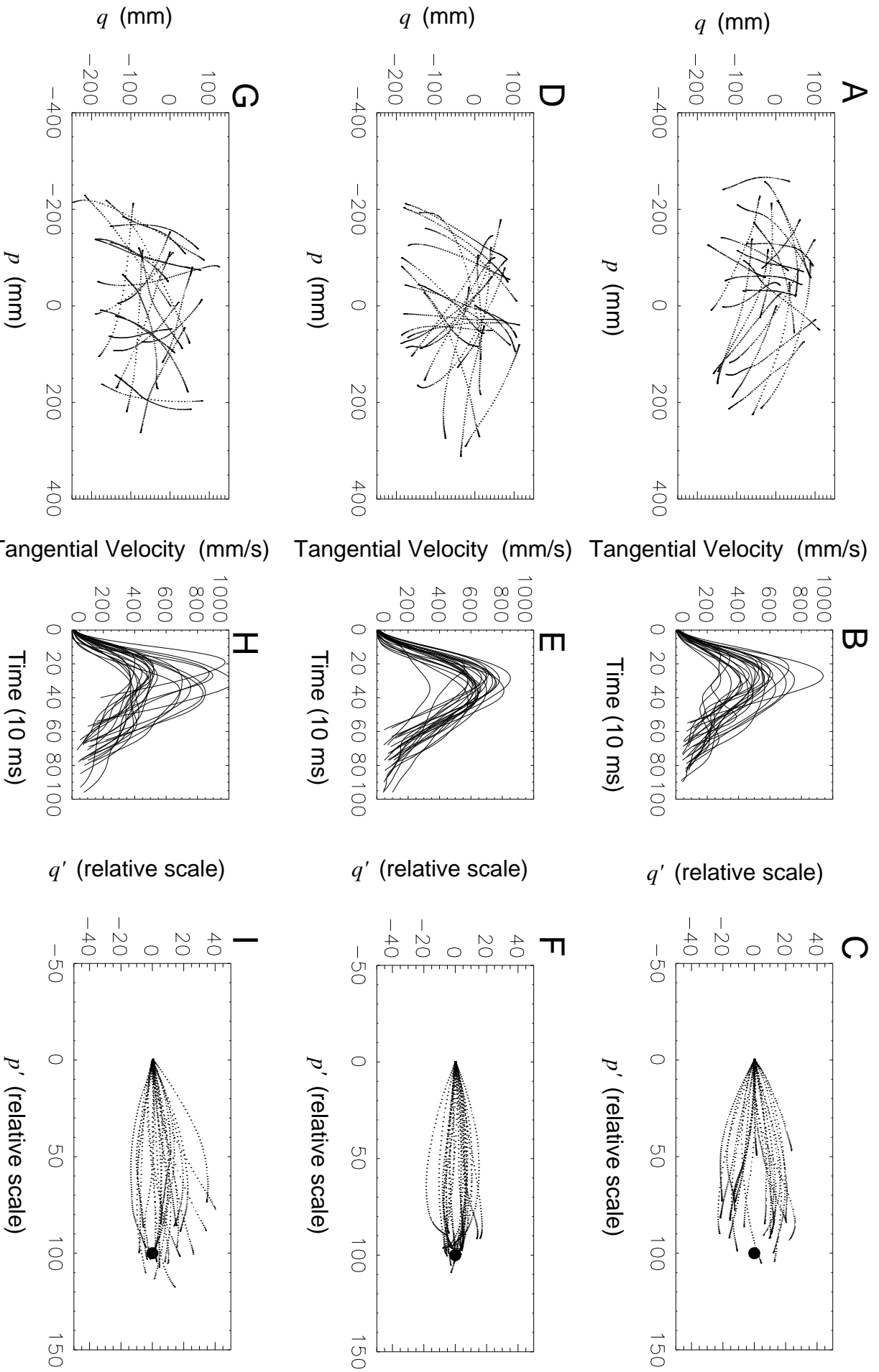


Fig. 11

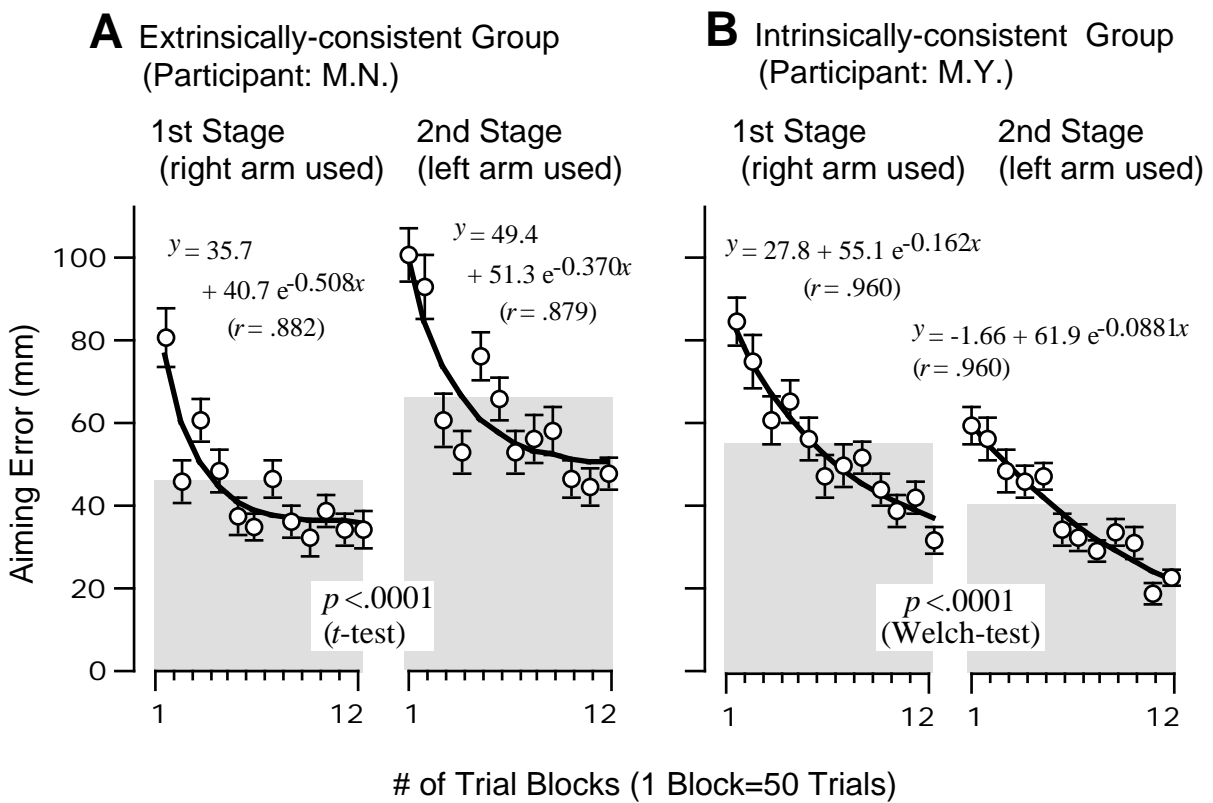


Fig. 12

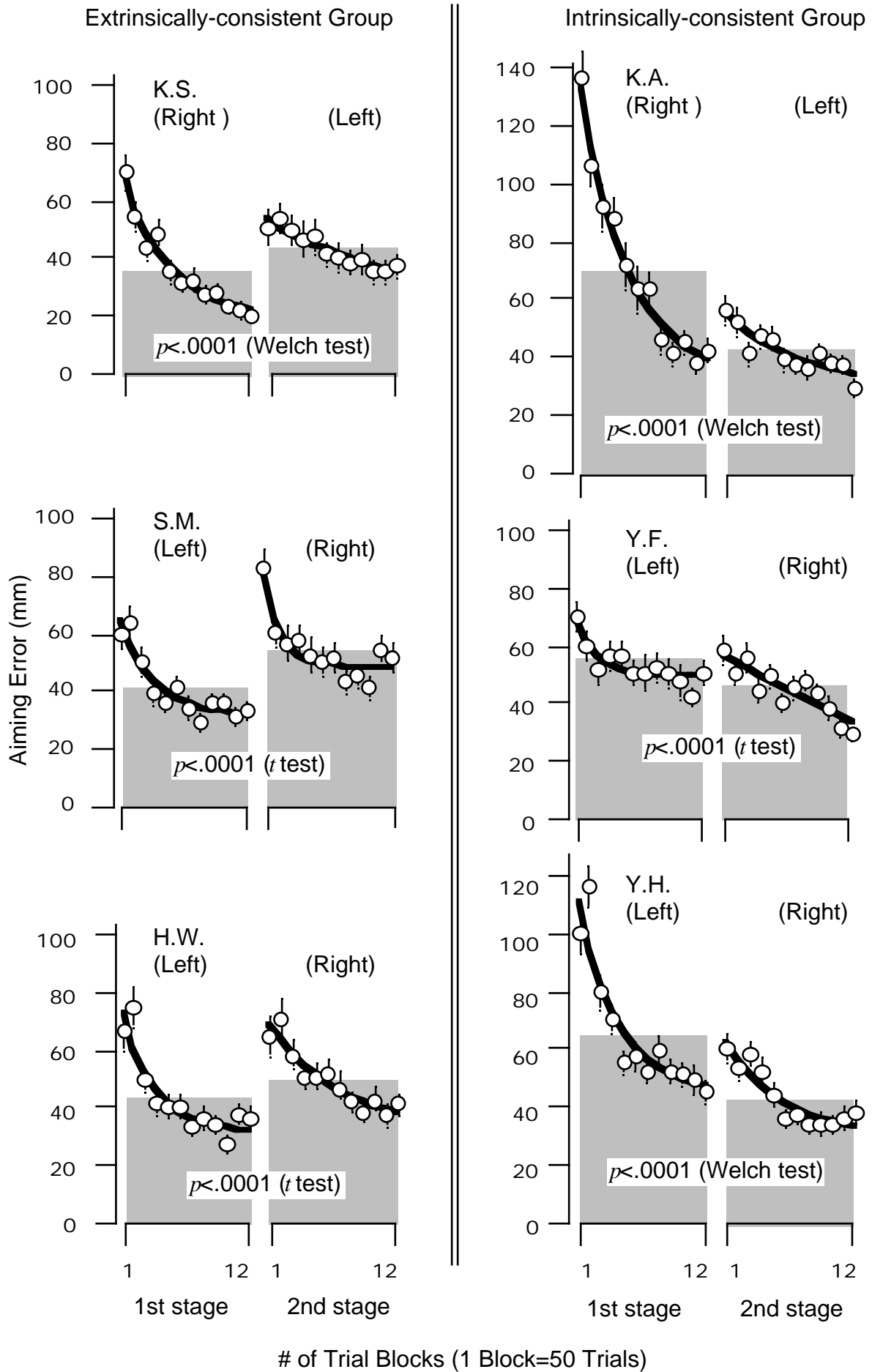


Fig.13

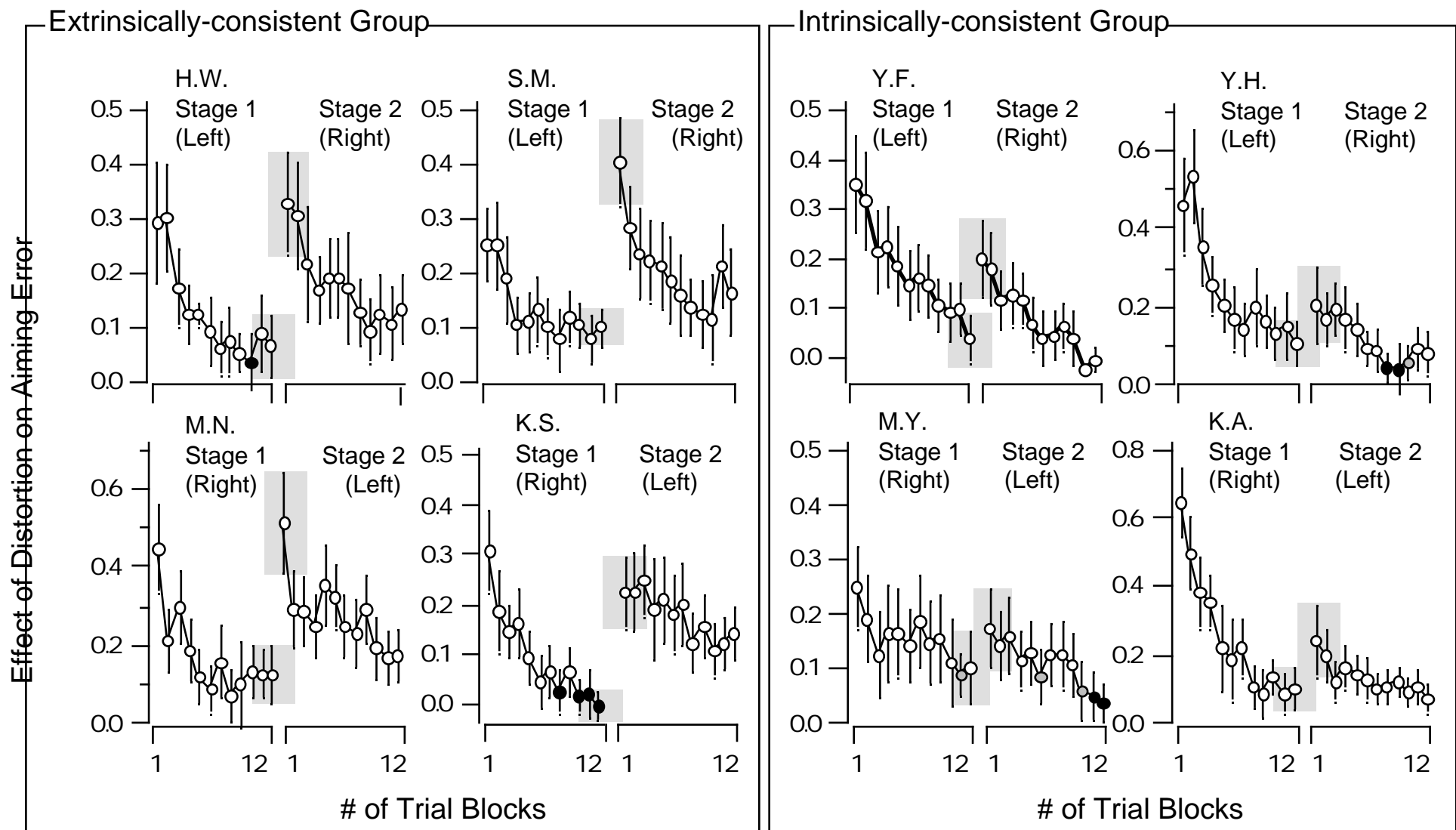


Fig. 14